
On Affine Homotopy between Language Encoders

Robin SM Chan^{1,*} Reda Boumasmoud¹ Anej Svete¹ Yuxin Ren²
 Qipeng Guo³ Zhijing Jin^{1,4} Shauli Ravfogel⁵ Mrinmaya Sachan¹
 Bernhard Schölkopf^{1,4} Mennatallah El-Assady¹ Ryan Cotterell¹
¹ETH Zürich ²Tsinghua University ³Fudan University
⁴Max Plank Institute for Intelligent Systems ⁵Bar-Ilan University

Abstract

Pre-trained language encoders—functions that represent text as vectors—are an integral component of many NLP tasks. We tackle a natural question in language encoder analysis: What does it mean for two encoders to be similar? We contend that a faithful measure of similarity needs to be *intrinsic*, that is, task-independent, yet still be informative of *extrinsic* similarity—the performance on downstream tasks. It is common to consider two encoders similar if they are *homotopic*, i.e., if they can be aligned through some transformation. In this spirit, we study the properties of *affine* alignment of language encoders and its implications on extrinsic similarity. We find that while affine alignment is fundamentally an asymmetric notion of similarity, it is still informative of extrinsic similarity. We confirm this on datasets of natural language representations. Beyond providing useful bounds on extrinsic similarity, affine intrinsic similarity also allows us to begin uncovering the structure of the space of pre-trained encoders by defining an order over them.²

1 Introduction

A common paradigm in modern natural language processing (NLP) is to pre-train a **language encoder** on a large swathe of natural language text. Then, a task-specific model is fit (*fine-tuned*) using the language encoder as the representation function of the text. More formally, a language encoder is a function $\mathbf{h}: \Sigma^* \rightarrow \mathbb{R}^d$, i.e., a function that maps a string over an alphabet Σ to a finite-dimensional vector. Now, consider sentiment analysis as an informative example of a task. Suppose our goal is to classify a string $\mathbf{y} \in \Sigma^*$ as one of three polarities $\Pi = \{\odot, \ominus, \oplus\}$. Then, the probability of \mathbf{y} exhibiting a specific polarity is often given by a log-linear model; e.g., the probability of \odot is

$$p(\odot | \mathbf{y}) = \text{softmax}(\mathbf{E} \mathbf{h}(\mathbf{y}) + \mathbf{b})_{\odot} \quad (1)$$

where $\mathbf{E} \in \mathbb{R}^{3 \times d}$, $\mathbf{b} \in \mathbb{R}^3$ and $\text{softmax}: \mathbb{R}^N \rightarrow \Delta^{N-1}$ is the softmax normalization function. Empirically, using a pre-trained encoder \mathbf{h} leads to significantly better classifier performance.

In the context of the widespread deployment of language encoders, this paper tackles a natural question: Given two language encoders \mathbf{h} and \mathbf{g} , how can we judge to what extent they are similar? This question is of practical importance; recent studies have shown that even small variations in the random seed used for training can result in significant performance differences on downstream tasks between models with the same architecture [12, 34]—that is, the models exhibit *extrinsic* differences. Such language encoders cannot be considered similar or used interchangeably despite their architectural similarities. Moreover, an elementary understanding also calls for an *intrinsic* (task-independent) measure of similarity—ideally, one that is informative about the extrinsic similarity on *any* downstream task we might be interested in.

*Corresponding author, robin.chan@inf.ethz.ch.

²Code will be published in the final version of the paper.

Symbol	Meaning	Introduced
d	Size of string representations.	§1
Δ^{N-1}	The $N - 1$ -dimensional probability simplex.	§1
V	\mathbb{R} -vector space.	§2
\mathcal{E}_V	\mathbb{R} -vector space of language encoders.	§2
$\text{Aff}(V)$	The set of (invertible) affine transformations on V .	§3.2
$\text{GL}(V)$	The set of invertible $d \times d$ real matrices.	§3.2
\mathfrak{d}_S	One-sided affine alignment measure over set $S \subseteq \text{Aff}(V)$.	Eq. (9b)
\mathfrak{d}_S	Two-sided affine alignment measure over set $S \subseteq \text{Aff}(V)$.	Remark 3.2
$d^{\mathcal{H}}$	Hausdorff-Hoare map for some map d .	Def. 3.3
\mathfrak{D}	Approximation of \mathfrak{d} for finite representation sets.	Eq. (18)
$D_{\psi'}$	Approximation of $d_{\infty, \Delta^{N-1}}(\text{softmax}_{\lambda}(\psi' \mathbf{h}), \mathcal{V}_N(\mathbf{g}))$ for finite representation sets.	Eq. (19)
\succsim	A preorder.	§4 & §5
\simeq	An equivalence relation.	§4
$[N] \subset \mathbb{N}$	The set $\{1, \dots, N\}$ for $N \in \mathbb{N}$.	§5

Table 1: A summary of notation used in the paper.

Rather than studying encoders directly, existing work investigates their similarity by studying the relationships between finite sets of representations [4, 19, 22, 41, *inter alia*]. Concretely, since language encoders are usually used by transforming the produced representations with a simple task-specific function (e.g., in a log-linear model as in Eq. (1)), it is natural to study transformations between pairs of encoders. For example, a line of work (implicitly) asserts that two language encoders are the same if they can be approximately *linearly aligned* [22, 27]: If there exists a linear transformation $\mathbf{A} \in \mathbb{R}^{d \times d}$ such that $\mathbf{h}(\mathbf{y}) \approx \mathbf{A}\mathbf{g}(\mathbf{y})$ for all strings $\mathbf{y} \in \mathcal{D}$ in some finite subset $\mathcal{D} \subset \Sigma^*$.³ In contrast, we set out to study the relationships between encoders, i.e., functions, themselves. This decision, rather than being just a technicality, allows us to derive a richer set of properties of their relationships than studying finite sets of representations. Concretely, we ask what notions of similarity between encoders one could consider and what they imply for their relationships.

The main contributions of the paper are of a theoretical nature. We first define an (extended) metric space on encoders. We then extend this definition to account for *transformations* in a broad framework of *S -homotopy* for a set of transformations S , where \mathbf{h} is S -homotopic to \mathbf{g} if \mathbf{h} can be transformed into \mathbf{g} through some transformation in S . As a concrete application of the framework, we study hemi-metrics for *affine* homotopy—the similarity of \mathbf{h} and $\psi \circ \mathbf{g}$ for affine transformations ψ . The notion of intrinsic similarity induced by such one-sided alignment is not symmetric. Nevertheless, we prove it to be informative of *extrinsic* similarity: If one encoder can be affinely mapped to another, we can theoretically guarantee that it also performs similarly on downstream tasks. We confirm this empirically by studying the intrinsic and extrinsic similarities of the 25 pre-trained MULTIBERT models [10, 34], where we observe a positive correlation between intrinsic and extrinsic similarity. Moreover, beyond measuring similarity, homotopy also allows us to define a form of hierarchy on the space of encoders, elucidating a clear structure in which some encoders are more informative than others. Such an order is also suggested by experiments, where we find that certain encoders are easier to map to than others.

2 Language Encoders

Let Σ be an alphabet⁴ of symbols y and $\text{EOS} \notin \Sigma$ a distinguished end-of-string symbol. By $\Sigma^* \stackrel{\text{def}}{=} \cup_{n=0}^{\infty} \Sigma^n$ we denote the Kleene closure of Σ , the set of all strings \mathbf{y} . A **language encoder** is a function $\mathbf{h}: \Sigma^* \rightarrow V \stackrel{\text{def}}{=} \mathbb{R}^d$ that maps strings to real vectors.⁵ Write $\mathcal{E}_V \stackrel{\text{def}}{=} V^{\Sigma^*}$ for the \mathbb{R} -vector space of language encoders, and $\mathcal{E}_b \subset \mathcal{E}_V$ its sub-vector space of **bounded encoders**.

³Related work is discussed in more detail in App. B.

⁴An alphabet is a finite, non-empty set.

⁵In principle, one could relax the replace \mathbb{R}^d with any finite dimensional vector space.

There are two common ways that language encoders are created. The first is through autoregressive language modeling. A **language model** (LM) is a probability distribution over Σ^* .⁶ **Autoregressive** LMs are defined through the multiplication of conditional probability distributions $p_{\mathbf{h}}(y_t \mid \mathbf{y}_{<t})$ as

$$p_{\mathbf{h}}^{\text{LM}}(\mathbf{y}) = p_{\mathbf{h}}(\text{EOS} \mid \mathbf{y}) \prod_{t=1}^T p_{\mathbf{h}}(y_t \mid \mathbf{y}_{<t}), \quad (2)$$

where each $p_{\mathbf{h}}(\cdot \mid \mathbf{y}_{<t})$ is a distribution over $\Sigma \cup \{\text{EOS}\}$ *parametrized* by a language encoder \mathbf{h} :

$$p_{\mathbf{h}}(y_t \mid \mathbf{y}_{<t}) \stackrel{\text{def}}{=} \text{softmax}(\mathbf{E} \mathbf{h}(\mathbf{y}_{<t}))_{y_t}, \quad (3)$$

where $\mathbf{E} \in \mathbb{R}^{(|\Sigma|+1) \times D}$. An autoregressive LM provides a simple manner to *learn* a language encoder from a dataset of strings $\mathcal{D} = \{\mathbf{y}^{(n)}\}_{n=1}^N$ by minimizing \mathcal{D} 's negative log-likelihood. We may also learn a language encoder through **masked language modeling** (MLM), which defines the conditional probabilities based on both sides of the masked symbol's context

$$p_{\mathbf{h}}(y_t \mid \mathbf{y}_{<t}, \mathbf{y}_{>t}) \stackrel{\text{def}}{=} \text{softmax}(\mathbf{E} \mathbf{h}(\mathbf{y}_{<t} \circ [\text{MASK}] \circ \mathbf{y}_{>t}))_{y_t}. \quad (4)$$

Optimizing the log-likelihood for a language encoder \mathbf{h} with a gradient-based algorithm only requires \mathbf{h} to be a differentiable function of its parameters. Once a language encoder has been trained on a (large) corpus, its representations can be used on more fine-grained NLP tasks such as classification. The rationale here is that representations $\mathbf{h}(\mathbf{y})$ stemming from a performant language model also contain information useful for other downstream tasks on natural language. An NLP practitioner might then implement a task-specific transformation of $\mathbf{h}(\mathbf{y})$. Since the tasks of interest are often less resource-abundant and to keep the training costs low, task-specific transformations are usually simple, often in the form of linear transformations of $\mathbf{h}(\mathbf{y})$, as in Eq. (1).

3 Affine Hemi-Metrics

As motivated in §1, we aim to characterize *affine* homotopy in the space of encoders. To this end, we first introduce various affine alignment measures and hemi-metrics on \mathcal{E}_V .

3.1 Preliminaries on Hemi-Metric Spaces

Note that to accommodate *unbounded encoders*, i.e., encoders that map to infinity, it will be convenient to allow distances and norms to take extended real numbers as values.⁷

Definition 3.1. An *extended metric* on a set X is a map $d: X \rightarrow \overline{\mathbb{R}}_+$ such that

- a. $\forall x, y \in X, \quad d(x, y) = 0$ iff $x = y$;
- b. (*Triangle Inequality*) $\forall x, y, z \in X, \quad d(x, y) \leq d(x, z) + d(z, y)$;
- c. (*Symmetry*) $\forall x, y \in X, \quad d(x, y) = d(y, x)$.

Similarly, an *extended norm* is a map $\|\cdot\|: X \rightarrow \overline{\mathbb{R}}_+$ that satisfies the norm axioms. In the upcoming sections, we will be considering maps d that do not satisfy the symmetry axiom. Lawvere [25] notes that symmetry is artificial and unnecessary for many of the main theorems involving metric spaces. In such situations, the quantity $d(x, y)$ can be interpreted as the “cost” of going from x to y . Occasionally, we want our distance to capture that it costs more to go from x to y than to return, making asymmetry desirable.

Definition 3.2. A *hemi-metric*⁸ or *Lawvere-metric* on a set X is a map $d: X \rightarrow \overline{\mathbb{R}}_+$ such that

- a. $d(x, x) = 0,$
- b. $d(x, z) \leq d(x, y) + d(y, z)$ for all $x, y, z \in X$.

⁶In the following, we assume language model *tightness* to the effect that we can assume that LMs produce valid probability distributions over Σ^* [14].

⁷ $\overline{\mathbb{R}}_+$ is the set of non-negative real numbers along with the “value” ∞ , assumed to be above all reals. We adopt the following conventions: $\infty \cdot 0 = 0 \cdot \infty = 0$; $\infty + r = r + \infty = \infty$ for every $r \in \mathbb{R}$; $\infty \cdot r = \mathbb{R}_{>0}$.

⁸A basic example of a hemi-metric space is the pair $(\mathbb{R}, d_{\mathbb{R}})$, where $d_{\mathbb{R}}(x, y) = \max(x - y, 0)$.

Definition 3.3. Let (X, d) be a hemi-metric space. For every non-empty $E \subset X$, we define the maps

$$d(x, E) \stackrel{\text{def}}{=} \inf_{y \in E} d(x, y) \quad (5) \quad \text{and} \quad d^{\mathcal{H}}(E, E') \stackrel{\text{def}}{=} \sup_{x \in E} d(x, E'). \quad (6)$$

The map $d^{\mathcal{H}}$ is called the **Hausdorff-Hoare map** and is a hemi-metric on $\mathcal{P}(X) \setminus \{\emptyset\}$, the power set of X . Additional properties of $d^{\mathcal{H}}$ are discussed in Lemma C.1.

Remark 3.1 (Hemi-Metric Recipe). Let X be any set, (Y, d) be a hemi-metric space and $S: X \rightarrow \mathcal{P}(Y) \setminus \{\emptyset\}$, $x \mapsto E_x$. Using Lemma C.1, we can construct a hemi-metric on X with $d_S^{\mathcal{H}}(x, y) \stackrel{\text{def}}{=} d^{\mathcal{H}}(E_x, E_y)$, and an **extended pseudo-metric** (that is, a symmetric hemi-metric) with $d_S^{\mathcal{H}}(x, y) = d_S^{\mathcal{H}^{\text{sym}}}(x, y) = \max(d_S^{\mathcal{H}}(x, y), d_S^{\mathcal{H}}(y, x))$.

Note that Remark 3.1 introduces a general recipe for defining hemi-metric spaces on some ‘‘function spaces’’. These are topological spaces whose elements are functions from a set to an extended-metric space. This naturally applies to the study of encoders and their transformations, which we call **S -homotopy**, i.e., two encoders are **S -homotopic** if one can be S -continuously deformed into the other. Given the space of encoders \mathcal{E}_V , we could, for example, take S as the set of all continuous maps, smooth maps, or multi-layer perceptrons. Our following discussion of affine maps, i.e., where $S = \text{Aff}(V)$, is extrinsically motivated but can be understood as a specific instance of the more general framework of S -homotopy.

3.2 Uniform Convergence Norm and Distance on \mathcal{E}_V

Given that all norms on the \mathbb{R} -vector space V are equivalent [24, Proposition 2.2 §XII], we may fix any norm $|\cdot|_V$ on V once and for all. We introduce the two maps $\|\cdot\|_{\infty}: \mathcal{E}_V \rightarrow \overline{\mathbb{R}}_+$ and $d_{\infty}(\cdot, \cdot): \mathcal{E}_V \times \mathcal{E}_V \rightarrow \overline{\mathbb{R}}_+$, given by

$$\|\mathbf{h}\|_{\infty} \stackrel{\text{def}}{=} \sup_{\mathbf{y} \in \Sigma^*} |\mathbf{h}(\mathbf{y})|_V \quad (7) \quad \text{and} \quad d_{\infty}(\mathbf{h}, \mathbf{g}) = \|\mathbf{h} - \mathbf{g}\|_{\infty}, \quad (8)$$

where $\|\cdot\|_{\infty}$ is an extended norm on \mathcal{E}_V and $(\mathcal{E}_V, d_{\infty})$ is a complete extended metric space.⁹

We write $\|\cdot\|_V: \text{GL}(V) \rightarrow \mathbb{R}_+$ for the subordinate matrix norm, i.e., $\|\mathbf{A}\|_V = \sup_{\mathbf{v} \in V \setminus \{0\}} \frac{|\mathbf{A}\mathbf{v}|_V}{|\mathbf{v}|_V}$. By abuse of language, we can view V as an affine space¹⁰ and set $\text{Aff}(V)$ for the group of affine transformations of V . An affine transformation ψ on V is a map $\mathbf{v} \mapsto \mathbf{A}\mathbf{v} + \mathbf{b}$, for some invertible $\mathbf{A} \in \text{GL}(V)$ and $\mathbf{b} \in V$. We call $\psi_{\text{lin}} \stackrel{\text{def}}{=} \mathbf{A}$ the linear part of ψ and $t_{\psi}: \mathbf{v} \mapsto \mathbf{v} + \mathbf{b}$ its translation part. Set $\mathcal{T} \subset \text{Iso}(V)$, for the subgroups of translations and affine isometries, respectively. Note that there is a natural action of $\text{Aff}(V)$ on \mathcal{E}_V , i.e., $\text{Aff}(V) \times \mathcal{E}_V \rightarrow \mathcal{E}_V$, $\mathbf{h} \mapsto \psi \circ \mathbf{h}$.

3.3 Affine Alignment Measures

The following discusses the possible approaches for affine alignment between two encoders $\mathbf{h}, \mathbf{g} \in \mathcal{E}_V$ using the recipe provided by Remark 3.1. Namely, for any subset $S \subset \text{Aff}(V)$ we can define

$$\|\mathbf{h}\|_S \stackrel{\text{def}}{=} d_{\infty}(0_{\mathcal{E}_V}, S(\mathbf{h})) = \inf_{\psi \in S} \|\psi \circ \mathbf{h}\|_{\infty}. \quad (9a)$$

$$\mathfrak{d}_S(\mathbf{h}, \mathbf{g}) \stackrel{\text{def}}{=} d_{\infty}(\mathbf{h}, S(\mathbf{g})) = \inf_{\psi \in S} \|\mathbf{h} - \psi \circ \mathbf{g}\|_{\infty}. \quad (9b)$$

Remark 3.2. We note that when $S = \text{Aff}(V)$, the map $d_{\text{Aff}(V)}(\mathbf{h}, \mathbf{g}) \stackrel{\text{def}}{=} \inf_{\psi, \psi' \in \text{Aff}(V)} \|\psi \circ \mathbf{h} - \psi' \circ \mathbf{g}\|_{\infty}$ is trivially zero by Corollary C.1. Further, $\mathfrak{d}_{\text{Aff}(V)}$ defined in Eq. (9b) is not a metric on \mathcal{E}_V .¹¹

In the case of affine isometries $\text{Iso}(V) = \{\psi \in \text{Aff}(V) \mid \psi_{\text{lin}} \in \text{O}(V)\}$ we show that the pair $(\mathcal{E}_V, \mathfrak{d}_{\text{Iso}(V)})$ constitutes an extended pseudo-metric space.

⁹This follows immediately from the fact that $|\cdot|_V$ is a norm and from the completeness of V .

¹⁰This amounts to ‘‘forgetting’’ the special role played by the zero vector.

¹¹See App. C.2 for a derivation.

Proposition 3.1. *The pair $(\mathcal{E}_V, \bar{d}_{\text{Iso}(V)})$ is an extended pseudo-metric space.*

Proof. in App. C.2. ■

4 Intrinsic Affine Homotopy

By introducing affine alignment between encoders we can now formalize homotopic relations on \mathcal{E}_V . To this end, we first derive the affine intrinsic preorder \succeq_{Aff} on the space of encoders.

Lemma 4.1. *Let (X, d) be a hemi-metric space. The relation $(x \succeq_d y \text{ iff } d(x, y) = 0)$ is a **preorder**¹² and it will be called the **specialization ordering** of d .*

Proof. Goubault-Larrecq [16, Proposition 6.1.8]. ■

Lemma 4.2 (Intrinsic Affine Preorder). *For any two encoders $\mathbf{h}, \mathbf{g} \in \mathcal{E}_V$, define the relation $(\mathbf{h} \succeq_{\text{Aff}} \mathbf{g} \text{ iff } \bar{d}_{\text{Aff}(V)}(\mathbf{h}, \mathbf{g}) = 0)$. Then \succeq_{Aff} is a preorder on \mathcal{E}_V .*

Proof. Follows from $\bar{d}_{\text{Aff}}(\psi \circ \mathbf{h}, \mathbf{g}) \leq \|\psi_{\text{lin}}\|_V \cdot \bar{d}_{\text{Aff}}(\mathbf{h}, \mathbf{g})$, see App. C.3. ■

To derive the implications of \succeq_{Aff} we first need to introduce the notion of an encoder rank.

Definition 4.1 (Encoder Rank). *For any $\mathbf{h} \in \mathcal{E}_V$ let the **encoder rank** be $\text{rank}(\mathbf{h}) \stackrel{\text{def}}{=} \dim_{\mathbb{R}}(V_{\mathbf{h}})$, where $V_{\mathbf{h}} \stackrel{\text{def}}{=} \langle \mathbf{h}(\Sigma^*) \rangle$ is the subvector space generated by the image of \mathbf{h} . When $\text{rank}(\mathbf{h}) = \dim_{\mathbb{R}}(V)$, \mathbf{h} is a full rank encoder, else it is rank deficient.*

Theorem 4.1. *Let $\mathbf{h}, \mathbf{g} \in \mathcal{E}_V$, we then have*

$$\mathbf{h} \succeq_{\text{Aff}} \mathbf{g} \Leftrightarrow \mathbf{h} = \psi(\pi_{\mathbf{h}}\mathbf{g}) \text{ for some } \psi \in \text{Aff}(V) \quad (10)$$

where, $\pi_{\mathbf{h}}$ is the orthogonal projection of V onto $V_{\mathbf{h}}$. In particular, if $\bar{d}_{\text{Aff}(V)}(\mathbf{h}, \mathbf{g}) = 0$ then $\text{rank}(\mathbf{h}) \leq \text{rank}(\mathbf{g})$. If in addition, we know $\text{rank}(\mathbf{g}) = \text{rank}(\mathbf{h})$, then \mathbf{g} must be an affine transformation of \mathbf{h} , i.e. $\mathbf{h} = \psi \circ \mathbf{g}$ for some $\psi \in \text{Aff}(V)$.

Proof. See App. C.3. ■

This allows us to state our first notion of language encoder similarity: intrinsic affine homotopy.

Definition 4.2 (Exact Intrinsic Affine Homotopy). *We say that two encoders $\mathbf{h}, \mathbf{g} \in \mathcal{E}_V$ are **exactly intrinsically affinely homotopic** and write $\mathbf{h} \simeq_{\text{Aff}} \mathbf{g}$ if*

$$\bar{d}_{\text{Aff}(V)}(\mathbf{h}, \mathbf{g}) = 0 \text{ and } \text{rank}(\mathbf{h}) = \text{rank}(\mathbf{g}). \quad (11)$$

For any $\mathbf{h}, \mathbf{g} \in \mathcal{E}_V$, one can easily show that

$$\mathbf{h} \simeq_{\text{Aff}} \mathbf{g} \iff \mathbf{g} \succeq_{\text{Aff}} \mathbf{h} \ \& \ \mathbf{h} \succeq_{\text{Aff}} \mathbf{g} \iff \bar{d}_{\text{Aff}(V)}^{\mathcal{H}^{\text{sym}}}(\mathbf{h}, \mathbf{g}) = 0, \quad (12)$$

which implies that \simeq_{Aff} is an equivalence relation on the set of language encoders \mathcal{E}_V .

5 Extrinsic Homotopy

We now extend the discussion from §4 to describe a principle for the *extrinsic* homotopy of language encoders. We argue that because the primary use case of language encoders is to perform transfer learning, as in the sentiment analysis example in §1, the main determining factor for whether two encoders are similar is how closely we can map their task prediction classification probabilities.

Definition 5.1 (Extrinsic Homotopy). *Two language encoders \mathbf{h} and \mathbf{g} are **extrinsically homotopic** if we can guarantee a similar performance on any downstream task \mathbf{h} and \mathbf{g} might be used for.*

¹²A reflexive and transitive relation on X .

The rest of the section formalizes this intuitive notion and describes its relationship with intrinsic affine homotopy. Let W be the vector space \mathbb{R}^N and set $\text{Aff}(V, W)$ as the set of affine maps from V to W .¹³ We define $\mathcal{E}_\Delta \stackrel{\text{def}}{=} \text{Map}(\Sigma^*, \Delta^{N-1})$ and $\mathcal{E}_W = \text{Map}(\Sigma^*, W)$. Lastly, we formalize the notion of a transfer learning task as a classifier using the language encoder representations. Particularly, we set \mathcal{V}_N to be the family of log-linear models as follows

$$\mathcal{V}_N: \mathcal{E}_V \rightarrow \mathcal{P}(\mathcal{E}_{\Delta^{N-1}}) \setminus \{\emptyset\}, \quad \mathbf{h} \mapsto \text{softmax}_\lambda(\text{Aff}_{V,W}(\mathbf{h})), \quad (13)$$

where $\text{Aff}_{V,W}$ is the map

$$\text{Aff}_{V,W}: \mathcal{E}_V \rightarrow \mathcal{P}(\mathcal{E}_W) \setminus \{\emptyset\}, \quad \mathbf{h} \mapsto \{\psi \circ \mathbf{h} \mid \psi \in \text{Aff}(V, W)\}. \quad (14)$$

Remark 5.1. Each $p_\psi = \text{softmax} \circ \psi(\mathbf{h}(\mathbf{y}))$ can be seen as a ‘‘probability distribution’’ over $[N]$

$$\mathcal{V}_N(\mathbf{h}) = \{p(\square \mid \mathbf{y}): [N] \rightarrow [0, 1], \square \mapsto \text{softmax} \circ \psi(\mathbf{h}(\mathbf{y}))_\square \mid \psi \in \text{Aff}(V, W)\}. \quad (15)$$

In line with Remark 3.1, we can define the following hemi-metrics on \mathcal{E}_V .

Definition 5.2. For any two encoders $\mathbf{h}, \mathbf{g} \in \mathcal{E}_V$, we define¹⁴

$$d_{\text{Aff}(V,W)}(\mathbf{h}, \mathbf{g}) \stackrel{\text{def}}{=} d_{\infty, W}^{\mathcal{H}}(\text{Aff}_{V,W}(\mathbf{h}), \text{Aff}_{V,W}(\mathbf{g})) \quad (16)$$

$$d_{\mathcal{V}(V,\Delta)}(\mathbf{h}, \mathbf{g}) \stackrel{\text{def}}{=} d_{\infty, \Delta^{N-1}}^{\mathcal{H}}(\mathcal{V}_N(\mathbf{h}), \mathcal{V}_N(\mathbf{g})) \quad (17)$$

Lemma 5.1. Let $\mathbf{h}, \mathbf{g} \in \mathcal{E}_V$. We have

1. There exists a constant $c(\lambda) > 0$ such that for any $\psi \in \text{Aff}(V, W)$

$$d_{\infty, \Delta^{N-1}}(\text{softmax}_\lambda(\psi \circ \mathbf{h}), \mathcal{V}_N(\mathbf{g})) \leq c(\lambda) \|\psi\|_{\text{lim}} \|\dot{d}_{\text{Aff}(V)}(\mathbf{h}, \mathbf{g})\}.$$

2. $d_{\mathcal{V}(V,\Delta)}(\mathbf{h}, \mathbf{g}) \leq c(\lambda) d_{\text{Aff}(V,W)}(\mathbf{h}, \mathbf{g})$.
3. $\dot{d}_{\text{Aff}(V)}(\mathbf{h}, \mathbf{g}) = 0 \Rightarrow d_{\text{Aff}(V,W)}(\mathbf{h}, \mathbf{g}) = 0 \Rightarrow d_{\mathcal{V}(V,\Delta)}(\mathbf{h}, \mathbf{g}) = 0$.

Proof. in App. C.4. ■

It is useful to consider what Def. 5.2 and Lemma 5.1 say. Eq. (17) provides an exact measure of *how different* two encoders are on any transfer learning task. This, therefore, formalizes the notion of extrinsic homotopy (cf. Def. 5.1), captured by the following definition.

Lemma 5.2 (Extrinsic Affine Preorder). *An encoder $\mathbf{h} \in \mathcal{E}_V$ is exactly extrinsically homotopic to¹⁵ $\mathbf{g} \in \mathcal{E}_V$ if $d_{\mathcal{V}(V,\Delta)}(\mathbf{h}, \mathbf{g}) = 0$. The relation $(\mathbf{h} \succeq_{\text{Ext}} \mathbf{g} \text{ iff } d_{\mathcal{V}(V,\Delta)}(\mathbf{h}, \mathbf{g}) = 0)$ is a preorder on \mathcal{E}_V .*

Proof. Follows from Lemma C.1. ■

Lemma 5.1 further shows that \succeq_{Ext} is *finer* than \succeq_{Aff} . This means that the affine intrinsic preorder is contained in the extrinsic preorder, i.e., $\mathbf{h} \succeq_{\text{Aff}} \mathbf{g} \Rightarrow \mathbf{h} \succeq_{\text{Ext}} \mathbf{g}$. Lastly, we can show that $d_{\mathcal{V}(V,\Delta)}(\mathbf{h}, \mathbf{g})$ is upper bounded by the intrinsic hemi-metric $d_{\text{Aff}(V)}^{\mathcal{H}}$.

Theorem 5.1 (ε -Intrinsic $\Rightarrow \mathcal{O}(\varepsilon)$ -Extrinsic). *Let $\mathbf{h}, \mathbf{g} \in \mathcal{E}_V$ be two encoders. Then,*

$$d_{\mathcal{V}(V,\Delta)}(\mathbf{h}, \mathbf{g}) \leq c(\lambda) d_{\text{Aff}(V)}^{\mathcal{H}}(\mathbf{h}, \mathbf{g}).$$

Proof. Follows from Lemma 5.1, in App. C.4. ■

¹³Given an affine map $f: V \rightarrow W$, there is a unique linear map $\mathbf{A} = f_{\text{lin}} \in \mathcal{L}(V, W)$ and $\mathbf{b} \in W$ such that for every $v \in V$ we have $f(v) = \mathbf{A} \cdot v + \mathbf{b}$.

¹⁴The subscript ∞ in $d_{\infty, \Delta}$ and $d_{\infty, W}$ is used to insist on that we are considering the supremum distance d_{∞} in Δ^{N-1} and W , respectively.

¹⁵Exact extrinsic homotopy is asymmetric.

6 Linear Alignment Methods for Finite Representation Sets

In practice, we can only measure the similarity of encoders in terms of the similarity of finite representation matrices $\mathbf{H}, \mathbf{G} \in \mathbb{R}^{N \times d}$ over a finite set of strings $\mathcal{Y} = \{\mathbf{y}^{(n)}\}_{n=1}^N$. In that case, we implement methods that approximate the notions of similarity discussed in §3 by optimizing over a finite set of affine maps $\psi \in \mathcal{A}_d \subset \text{Aff}(V)$ generally using gradient descent. Let $\mathbf{H}_{\mathbf{y},\cdot}, \mathbf{G}_{\mathbf{y},\cdot} \in \mathbb{R}^d$ be two encoder representations of string $\mathbf{y} \in \mathcal{Y}$. We implement intrinsic similarity by finding $\hat{\psi} \in \mathcal{A}_d$ that best maps \mathbf{G} to \mathbf{H} and reporting the maximum error as follows

$$\mathfrak{D}(\mathbf{H}, \mathbf{G}) \stackrel{\text{def}}{=} \min_{\psi \in \mathcal{A}_d} \max_{\mathbf{y} \in \mathcal{Y}} \|\mathbf{H}_{\mathbf{y},\cdot} - \psi \circ \mathbf{G}_{\mathbf{y},\cdot}\|_V, \quad (18)$$

and the extrinsic similarity measure for some fixed ψ'

$$D_{\psi'}(\mathbf{H}, \mathbf{G}) \stackrel{\text{def}}{=} \min_{\psi \in \mathcal{A}_d} \max_{\mathbf{y} \in \mathcal{Y}} \|\text{softmax}(\psi' \circ \mathbf{H}_{\mathbf{y},\cdot}) - \text{softmax}(\psi \circ \mathbf{G}_{\mathbf{y},\cdot})\|_V, \quad (19)$$

where ψ' may be learned through task fine-tuning. Several commonly used linear alignment methods provide solutions to related optimization problems as in Eq. (18), which we review in the following.

Orthogonal Procrustes Problem. We can find the orthogonal transformation that minimizes the Frobenius norm between representations by solving the orthogonal Procrustes problem [33]:

$$\underset{\mathbf{A} \in \mathcal{A}_d}{\text{argmin}} \|\mathbf{H} - \mathbf{A}\mathbf{G}\|_F, \quad \text{s.t. } \mathbf{A}^\top \mathbf{A} = \mathbb{I}. \quad (20)$$

Given the singular-value decomposition $\mathbf{H}^\top \mathbf{G} = \mathbf{U}\Sigma\mathbf{V}^\top$, the solution to Eq. (20) is $\mathbf{U}\mathbf{V}^\top$.¹⁶ The goodness of fit is then reported as $\|\mathbf{H} - \mathbf{U}\mathbf{V}\mathbf{G}\|_F$. Note that Eq. (20) discusses linear alignment for isometries, which, by Prop. 3.1, defines an extended pseudo-metric space.

Canonical Correlation Analysis (CCA). CCA [19] is a linear alignment method which finds the matrices \mathbf{A}, \mathbf{B} that project \mathbf{H} and \mathbf{G} into subspaces maximizing their canonical correlation. Let $\mathbf{A}_{\cdot,j}$ and $\mathbf{B}_{\cdot,j}$ be the j th column vectors of \mathbf{A} and \mathbf{B} , respectively. The formulation is as follows

$$\rho_j = \max_{\mathbf{A}_{\cdot,j}, \mathbf{B}_{\cdot,j}} \text{corr}(\mathbf{H}\mathbf{A}_{\cdot,j}, \mathbf{G}\mathbf{B}_{\cdot,j}) \quad \text{s.t.} \quad \forall_{i < j} \mathbf{H}\mathbf{A}_{\cdot,i} \perp \mathbf{H}\mathbf{A}_{\cdot,j}, \quad \forall_{i < j} \mathbf{G}\mathbf{B}_{\cdot,i} \perp \mathbf{G}\mathbf{B}_{\cdot,j}. \quad (21)$$

The representation similarity is measured in terms of the goodness of CCA fit, e.g., the mean squared CCA correlation $R_{\text{CCA}}^2 = \sum_{i=1}^d \rho_i^2 / d$. Note that we can reformulate the CCA objective in Eq. (21) as

$$\min_{\mathbf{A}, \mathbf{B}} \frac{1}{2} \|\mathbf{A}^\top \mathbf{H} - \mathbf{B}^\top \mathbf{G}\|_F^2 \quad \text{s.t.} \quad (\mathbf{A}^\top \mathbf{H})(\mathbf{A}^\top \mathbf{H})^\top = (\mathbf{B}^\top \mathbf{G})(\mathbf{B}^\top \mathbf{G})^\top = \mathbb{I}. \quad (22)$$

Given the singular-value decomposition $\mathbf{H}^\top \mathbf{G} = \mathbf{U}\Sigma\mathbf{V}^\top$, the solution of Eq. (22) is $(\hat{\mathbf{A}}, \hat{\mathbf{B}}) = ((\mathbf{H}\mathbf{H}^\top)^{-\frac{1}{2}}\mathbf{U}, (\mathbf{G}\mathbf{G}^\top)^{-\frac{1}{2}}\mathbf{V})$, where $(\mathbf{H}\mathbf{H}^\top)^{-\frac{1}{2}}$ and $(\mathbf{G}\mathbf{G}^\top)^{-\frac{1}{2}}$ are whitening transforms and \mathbf{U} and \mathbf{V} . Assuming the data is whitened during pre-processing, CCA corresponds to linear alignment under an orthogonality constraint, equivalent to the orthogonal Procrustes problem.¹⁷

CCA Extensions.¹⁸ Projection-weighted CCA (PWCCA) [29] also finds linear alignment matrices through CCA, but applies weighting to correlation values ρ_i to report the goodness of fit. Given the canonical vectors $\hat{\mathbf{A}}$, PWCCA reports $\hat{\rho}_{\text{PW}} = \sum_{i=1}^d \alpha_i \rho_i / \sum_i \alpha_i$, where $\alpha_i = \sum_j |\langle \hat{\mathbf{A}}_{\cdot,i}, \mathbf{H}_{\cdot,j} \rangle|$.

Non-Alignment Methods. CKA [22] evaluates kernel similarity between representations, however, its objective is not linear alignment. CKA computes the normalized Hilbert-Schmidt independence criterion [17] between centered kernel matrices $\mathbf{K}^{\mathbf{H}}$ and $\mathbf{K}^{\mathbf{G}}$ where $\mathbf{K}_{ij}^{\mathbf{H}} = k(\mathbf{H}_{i,\cdot}, \mathbf{H}_{j,\cdot})$, and $\mathbf{K}_{ij}^{\mathbf{G}} = k(\mathbf{G}_{i,\cdot}, \mathbf{G}_{j,\cdot})$ for any kernel function k , i.e., $\text{tr}(\mathbf{K}^{\mathbf{H}}\mathbf{K}^{\mathbf{G}}) / \sqrt{(\text{tr}(\mathbf{K}^{\mathbf{H}}\mathbf{K}^{\mathbf{H}})\text{tr}(\mathbf{K}^{\mathbf{G}}\mathbf{K}^{\mathbf{G}}))}$. We report the commonly used linear CKA, where $k(\mathbf{H}_{i,\cdot}, \mathbf{H}_{j,\cdot}) = \mathbf{H}_{i,\cdot}^\top \mathbf{H}_{j,\cdot}$.

¹⁶See App. D for the derivation.

¹⁷See App. D for further detail.

¹⁸CCA extensions beyond PWCCA are mentioned in App. B.

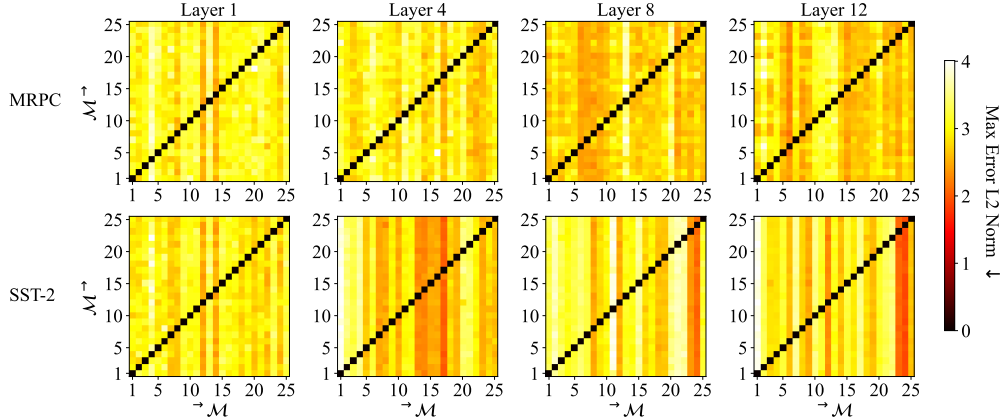


Figure 1: Asymmetry between MULTIBERT encoders across layers. For each pair of the 25 MULTIBERTs $\mathcal{M}^{(i)}$ and $\mathcal{M}^{(j)}$, we generate training set embeddings $\mathbf{H}^{(i)}, \mathbf{H}^{(j)} \in \mathbb{R}^{N \times d}$ for both MRPC and SST-2. We then fit $\mathbf{H}^{(i)}$ to $\mathbf{H}^{(j)}$ with an affine map and report the goodness of fit through the max error L2 norm, i.e., an approximation of $\mathfrak{D}(\mathbf{H}^{(j)}, \mathbf{H}^{(i)})$ on row i and column j of the grid.

7 Experiments

In this section, we explore the practical implications of our findings about the affine relations between encoders as measured by Eq. (18) and Eq. (19). For this purpose, we conduct experiments on the 25 MULTIBERT [34] encoders, which are architecturally identical to BERT-BASE [10] models pre-trained with different seeds. We report results on the training sets of two GLUE benchmark classification tasks; SST-2 [37] and MRPC [13]. When reporting \mathfrak{D} and $D_{\psi'}$ from Eq. (18) and Eq. (19), we use the L_2 norm for simplicity. We further provide a discussion of $d_{\mathcal{V}(V, \Delta)}$ by approximating¹⁹ the outer supremum as a maximum over a finite set of affine maps $\mathcal{A}_{d'} \subset \text{Aff}(\mathbb{R}^d)$ as

$$D^{\mathcal{H}}(\mathbf{H}, \mathbf{G}) \approx \max_{\psi' \in \mathcal{A}_{d'}} \min_{\psi \in \mathcal{A}_d} \max_{\mathbf{y} \in \mathcal{Y}} \|\text{softmax}(\psi' \circ \mathbf{H}_{\mathbf{y}, \cdot}) - \text{softmax}(\psi \circ \mathbf{G}_{\mathbf{y}, \cdot})\|_2. \quad (23)$$

The experimental setup and compute resources are further described in App. E.

The Intrinsic ‘Preorder’ of Encoders. We first investigate whether the asymmetry of $\mathfrak{d}_{\text{Aff}(V)}$ is measurable in the finite alphabet representations of MULTIBERT encoders. Figure 1 shows distinct vertical lines for both tasks indicating that there are encoders that are consistently easier to affinely map to ($\rightarrow \mathcal{M}$). This seems to be rather independent of which encoder we map from ($\mathcal{M} \rightarrow$). We further see that this trend is task-independent for early layers but diverges for later layers.

The Influence of Encoder Rank Deficiency. As discussed in §4, the encoder rank plays a pivotal role in affine mappability; exact affine homotopy is only achievable between equal-rank encoders.²⁰ With this in mind, we return to our findings from Figure 1 to evaluate whether the observed differences between encoders can be attributed to a difference in measurable rank. Due to the inaccuracies of computing the rank numerically, we approximate the encoder rank using the **rank to precision** ϵ as the number of representation matrix singular values larger than some $\epsilon \in \mathbb{R}$.²¹ We find statistically significant (p -value < 0.05 , assuming independence) rank correlation with the median intrinsic distance \mathfrak{D} when mapping *to* the corresponding encoder of $\rho_{\text{MRPC}} = 0.560$ and $\rho_{\text{SST2}} = 0.427$. We find no statistically significant correlations with the median distance when mapping *from* the corresponding encoder. This difference in encoder ranks could, therefore, partially explain the previously observed differences in affine mappability as some encoders seem to learn lower-rank representations.

¹⁹We discuss this and other limitations in App. A.

²⁰We provide additional experiments on the role of the encoder rank in App. F.

²¹A commonly used value for ϵ is $\sigma_1 \cdot \epsilon_p \cdot \max(N, d)$ [30], where σ_1 is the largest singular value of the $N \times d$ representation matrix and ϵ_p the float machine epsilon.

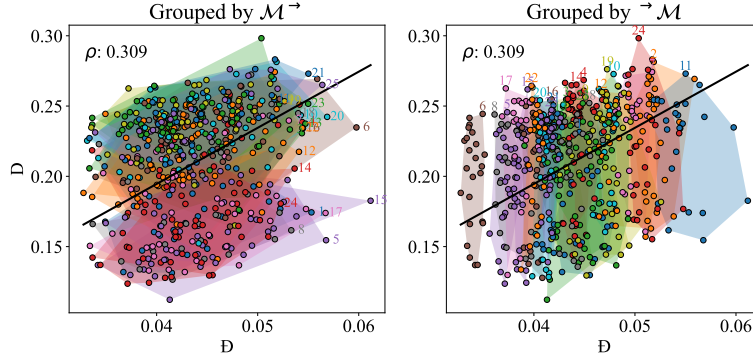


Figure 2: MRPC extrinsic ($D_{\psi'}$) against affine intrinsic (\mathfrak{D}) similarity, grouped by \mathcal{M}^{-1} (left), and $\vec{\mathcal{M}}$ (right). We additionally fit a linear regression from \mathfrak{D} to $D_{\psi'}$ as $D_{\psi'} = 3.992 \cdot \mathfrak{D} + 0.035$ to find the slope coefficient. The slope coefficient is significant at $p < 0.01$, with a standard error of 0.160.

A Linear Bound on Extrinsic Similarity. Lemma 5.1 derives a relationship between affine intrinsic and extrinsic similarity. To evaluate its strength in practice, we measure Spearman’s Rank Correlation (ρ) and Pearson Correlation (PCC) between intrinsic measures introduced in §6 and the extrinsic measures $D_{\psi'}$ and $D^{\mathcal{H}}$. PCC measures the strength and direction of a linear relationship between two random variables, whereas Spearman’s ρ additionally evaluates the variables’ monotonic association. $D_{\psi'}$ is computed by training a linear classifier $\psi' \in \text{Aff}(V)$ on the final MULTIBERT layer for each task. Further, we report $D^{\mathcal{H}}$ as the maximum L_2 loss for a large number of randomly generated²² classifiers ψ' on the final layer of each MULTIBERT. We generate 1000 such classifiers for $\mathcal{Y}_{\text{MRPC}}$ and 100 for $\mathcal{Y}_{\text{SST-2}}$.²³ Table 2 show significant, large linear correlation prevalent in all linear alignment methods, whereas CKA—a linear, non-alignment method—does not capture extrinsic behavior as faithfully. Further, Figure 2 visualizes the linear relationship explicitly for MRPC.

Intrinsic Measure		\mathfrak{D}	Orthogonal Procrustes	R_{CCA}^2	PWCCA	Linear CKA	
Lin. Alignment-Based		Yes	Yes	Yes	Yes	No	
SST-2	$D_{\psi'}$	ρ	0.110*	0.095	0.172*	0.015	0.088
		PCC	0.768*	0.937*	0.932*	0.970*	0.231*
	$D^{\mathcal{H}}$	ρ	0.595*	0.107*	0.056	0.138*	0.179*
		PCC	0.692*	0.624*	0.609*	0.658*	0.173*
MPRC	$D_{\psi'}$	ρ	0.309*	0.250*	0.001	0.220*	0.214*
		PCC	0.707*	0.697*	0.733*	0.743*	0.241*
	$D^{\mathcal{H}}$	ρ	0.231*	0.025*	0.178*	0.059	0.030
		PCC	0.790*	0.755*	0.879*	0.875*	0.174*

Table 2: Spearman’s Rank Correlation Coefficient (ρ) and Pearson’s Correlation Coefficient (PCC) between common intrinsic measures and the extrinsic similarities $D_{\psi'}$ and $D^{\mathcal{H}}$ across datasets. * indicates a p -value < 0.01 (assuming independence).

8 Discussion

Implications of §5. Lemma 5.1 shows for any *fixed* affine transformation ψ' , the extrinsic dissimilarity $d_{\infty, \Delta^{N-1}}(\text{softmax}_{\lambda}(\psi' \circ \mathbf{h}), \mathcal{V}_N(\mathbf{g}))$ is linearly bounded by the intrinsic measure $\mathfrak{d}_{\text{Aff}(V)}(\mathbf{h}, \mathbf{g})$. Thm. 5.1 discusses a stronger bound, namely on the *worst-case* extrinsic dissimilarity among all downstream linear classifiers. Similar relationships can be observed empirically across

²²The generation process is described in App. E.

²³The computational expense of computing $D^{\mathcal{H}}$ restricts this analysis to a limited set of classifiers, depending on the alphabet size. See App. A for a discussion.

MULTIBERTs (cf. Tab. 2). Notably, it is commonly known that BERTs with different pre-training initialization perform differently across downstream tasks [28]. Whereas other similarity measures are tested to be *invariant* to such changes, e.g., in the seed specificity test [11], we show that intrinsic affine homotopy measures are rightfully *sensitive* to them.

Hemi-Metrics. We extend previous works of similarity between finite representation sets (cf. App. B) to notions of similarity between encoder *maps* to more formally characterize affine alignment measures on the space of encoders under the general framework of S -homotopy. Our formulation of the problem allows us to derive homotopic attributes, such as proper preorders between encoder maps. Although encoders are not exactly linearly related in practice, such notions of affine ‘order’ surface empirically, as highlighted in §7. Our discussion of hemi-metrics is related to the line of work surrounding similarity measures that operate in proper metric spaces [4, 35, 41]. However, hemi-metrics additionally capture asymmetries that characterize the space of encoders, as discussed in the following paragraph.

Affine Asymmetry in the Space of Encoders. The experimental results in §7 raise new questions about the landscape of pre-trained encoders. The asymmetry in the intrinsic affine similarity between similarly pre-trained encoders shown in Fig. 1 has implications on downstream task performance by Lemma 5.1 and the empirical results in Tab. 2. The fact that the same encoders seem to learn representations of different ranks to precision ϵ only offers a partial explanation, since mapping between artificially generated differently rank-deficient encoders yields mostly symmetric affine distances (cf. Fig. 3). Mathematically, one could imagine a potential explanation to be that easy-to-learn encoders are approximately linear expressions of others, making them easy to map *to*, but not necessarily *from*. We leave this to future work to explore. Overall, our empirical findings imply the need to consider associating directionality with encoder similarity to account for the apparent asymmetry of the problem.

9 Conclusion

We discuss language encoder similarity in the framework of S -homotopy. More specifically, we characterize various notions of affine alignment between encoder maps and prove that some provide desirable theoretical upper bounds on downstream task performance dissimilarity. Experiments show our notion of intrinsic affine homotopy to be consistently predictive of downstream task behavior while revealing an asymmetric order in the space of encoders.

Broader Impact

This paper presents foundational research about the similarity of language encoders. To the best of our knowledge, there are no ethical or negative societal implications to this work.

Acknowledgements

Ryan Cotterell acknowledges support from the Swiss National Science Foundation (SNSF) as part of the “The Forgotten Role of Inductive Bias in Interpretability” project. Anej Svete is supported by the ETH AI Center Doctoral Fellowship. Robin Chan acknowledges support from FYAYC. We thank Raphaël Baur and Furuì Cheng for helpful discussions and reviews of the current manuscript.

References

- [1] Guillaume Alain and Yoshua Bengio. 2017. Understanding intermediate layers using linear classifier probes. In *5th International Conference on Learning Representations, ICLR 2017, Workshop Track Proceedings*, Toulon, France.
- [2] Yamini Bansal, Preetum Nakkiran, and Boaz Barak. 2021. Revisiting model stitching to compare neural representations. In *Neural Information Processing Systems*.

- [3] Saaid Baraty, Dan A. Simovici, and Catalin Zara. 2011. The impact of triangular inequality violations on medoid-based clustering. In *Foundations of Intelligent Systems*, pages 280–289, Berlin, Heidelberg. Springer Berlin Heidelberg.
- [4] Enric Boix-Adserà, Hannah Lawrence, George Stepaniants, and Philippe Rigollet. 2024. GULP: A prediction-based metric between representations. In *Proceedings of the 36th International Conference on Neural Information Processing Systems, NIPS '22*, Red Hook, NY, USA. Curran Associates Inc.
- [5] Dmitri Burago, Yuri Burago, and Sergei Ivanov. 2001. *A Course in Metric Geometry*. American Mathematical Society, Providence, RI.
- [6] C. Chang, W. Liao, Y. Chen, and L. Liou. 2016. A mathematical theory for clustering in metric spaces. *IEEE Transactions on Network Science and Engineering*, 3(01):2–16.
- [7] Adrián Csiszárík, Péter Korösi-Szabó, Ákos K. Matszangosz, Gergely Papp, and Dániel Varga. 2021. Similarity and matching of neural network representations. In *Neural Information Processing Systems*.
- [8] Alexander D’Amour, Katherine A. Heller, Dan I. Moldovan, Ben Adlam, Babak Alipanahi, Alex Beutel, Christina Chen, Jonathan Deaton, Jacob Eisenstein, Matthew D. Hoffman, Farhad Hormozdiari, Neil Houlsby, Shaobo Hou, Ghassen Jerfel, Alan Karthikesalingam, Mario Lucic, Yi-An Ma, Cory Y. McLean, Diana Mincu, Akinori Mitani, Andrea Montanari, Zachary Nado, Vivek Natarajan, Christopher Nielson, Thomas F. Osborne, Rajiv Raman, Kim Ramasamy, Rory Sayres, Jessica Schrouff, Martin G. Seneviratne, Shannon Sequeira, Harini Suresh, Victor Veitch, Max Vladymyrov, Xuezhi Wang, Kellie Webster, Steve Yadlowsky, Taedong Yun, Xiaohua Zhai, and D. Sculley. 2020. Underspecification presents challenges for credibility in modern machine learning. *J. Mach. Learn. Res.*, 23:226:1–226:61.
- [9] Sanjoy Dasgupta and Philip M. Long. 2005. Performance guarantees for hierarchical clustering. *Journal of Computer and System Sciences*, 70(4):555–569. Special Issue on COLT 2002.
- [10] Jacob Devlin, Ming-Wei Chang, Kenton Lee, and Kristina Toutanova. 2019. BERT: Pre-training of deep bidirectional transformers for language understanding. In *Proceedings of the 2019 Conference of the North American Chapter of the Association for Computational Linguistics: Human Language Technologies, Volume 1 (Long and Short Papers)*, pages 4171–4186, Minneapolis, Minnesota. Association for Computational Linguistics.
- [11] Frances Ding, Jean-Stanislas Denain, and Jacob Steinhardt. 2021. Grounding representation similarity with statistical testing. *ArXiv*, abs/2108.01661.
- [12] Jesse Dodge, Gabriel Ilharco, Roy Schwartz, Ali Farhadi, Hannaneh Hajishirzi, and Noah Smith. 2020. Fine-tuning pretrained language models: Weight initializations, data orders, and early stopping.
- [13] William B. Dolan and Chris Brockett. 2005. Automatically constructing a corpus of sentential paraphrases. In *Proceedings of the Third International Workshop on Paraphrasing (IWP2005)*.
- [14] Li Du, Lucas Torroba Hennigen, Tiago Pimentel, Clara Meister, Jason Eisner, and Ryan Cotterell. 2023. A measure-theoretic characterization of tight language models. In *Proceedings of the 61st Annual Meeting of the Association for Computational Linguistics (Volume 1: Long Papers)*, pages 9744–9770, Toronto, Canada. Association for Computational Linguistics.
- [15] Bolin Gao and Laca Pavel. 2017. On the properties of the softmax function with application in game theory and reinforcement learning. *ArXiv*, abs/1704.00805.
- [16] Jean Goubault-Larrecq. 2013. *Metrics, quasi-metrics, hemi-metrics*, New Mathematical Monographs, page 203–259. Cambridge University Press.
- [17] Arthur Gretton, Olivier Bousquet, Alex Smola, and Bernhard Schölkopf. 2005. Measuring statistical dependence with Hilbert-Schmidt norms. In *Algorithmic Learning Theory*, pages 63–77, Berlin, Heidelberg. Springer Berlin Heidelberg.

- [18] William L. Hamilton, Jure Leskovec, and Dan Jurafsky. 2016. Diachronic word embeddings reveal statistical laws of semantic change. In *Proceedings of the 54th Annual Meeting of the Association for Computational Linguistics (Volume 1: Long Papers)*, pages 1489–1501, Berlin, Germany. Association for Computational Linguistics.
- [19] David Roi Hardoon, Sándor Szedmák, and John Shawe-Taylor. 2004. Canonical correlation analysis: An overview with application to learning methods. *Neural Computation*, 16:2639–2664.
- [20] Dieuwke Hupkes and Willem Zuidema. 2018. Visualisation and ‘diagnostic classifiers’ reveal how recurrent and recursive neural networks process hierarchical structure (extended abstract). In *Proceedings of the Twenty-Seventh International Joint Conference on Artificial Intelligence, IJCAI-18*, pages 5617–5621. International Joint Conferences on Artificial Intelligence Organization.
- [21] Max Klabunde, Tobias Schumacher, Markus Strohmaier, and Florian Lemmerich. 2023. Similarity of neural network models: A survey of functional and representational measures.
- [22] Simon Kornblith, Mohammad Norouzi, Honglak Lee, and Geoffrey Hinton. 2019. Similarity of neural network representations revisited. In *Proceedings of the 36th International Conference on Machine Learning*, volume 97 of *Proceedings of Machine Learning Research*, pages 3519–3529. PMLR.
- [23] Nikolaus Kriegeskorte, Marieke Mur, and Peter Bandettini. 2008. Representational similarity analysis - connecting the branches of systems neuroscience. *Frontiers in Systems Neuroscience*, 2.
- [24] Serge Lang. 2002. Algebra.
- [25] F. W. Lawvere. 2002. Metric spaces, generalized logic, and closed categories. *Theory and Applications of Categories No. 1 (2002) pp 1-37*.
- [26] Karel Lenc and Andrea Vedaldi. 2019. Understanding image representations by measuring their equivariance and equivalence. *International Journal of Computer Vision*, 127(5):456–476.
- [27] Li, Yixuan and Yosinski, Jason and Clune, Jeff and Lipson, Hod and Hopcroft, John. 2015. Convergent learning: Do different neural networks learn the same representations? In *Proceedings of the 1st International Workshop on Feature Extraction: Modern Questions and Challenges at NIPS 2015*, volume 44 of *Proceedings of Machine Learning Research*, pages 196–212, Montreal, Canada. PMLR.
- [28] R. Thomas McCoy, Junghyun Min, and Tal Linzen. 2020. BERTs of a feather do not generalize together: Large variability in generalization across models with similar test set performance. In *Proceedings of the Third BlackboxNLP Workshop on Analyzing and Interpreting Neural Networks for NLP*, pages 217–227, Online. Association for Computational Linguistics.
- [29] Ari S. Morcos, Maithra Raghu, and Samy Bengio. 2018. Insights on representational similarity in neural networks with canonical correlation. In *Neural Information Processing Systems*.
- [30] William H Press, Saul A Teukolsky, William T Vetterling, and Brian P Flannery. 2007. *Numerical Recipes: The Art of Scientific Computing*, 3rd edition. Cambridge University Press.
- [31] Maithra Raghu, Justin Gilmer, Jason Yosinski, and Jascha Sohl-Dickstein. 2017. SVCCA: Singular vector canonical correlation analysis for deep learning dynamics and interpretability. In *Proceedings of the 31st International Conference on Neural Information Processing Systems, NIPS’17*, page 6078–6087, Red Hook, NY, USA. Curran Associates Inc.
- [32] Yuxin Ren, Qipeng Guo, Zhijing Jin, Shauli Ravfogel, Mrinmaya Sachan, Bernhard Schölkopf, and Ryan Cotterell. 2023. All roads lead to rome? exploring the invariance of transformers’ representations.
- [33] Peter H. Schönemann. 1966. A generalized solution of the orthogonal procrustes problem. *Psychometrika*, 31(1):1–10.

- [34] Thibault Sellam, Steve Yadlowsky, Jason Wei, Naomi Saphra, Alexander D’Amour, Tal Linzen, Jasmijn Bastings, Iulia Turc, Jacob Eisenstein, Dipanjan Das, et al. 2022. The MultiBERTs: BERT reproductions for robustness analysis. In *ICLR*. OpenReview.net.
- [35] Mahdiyaz Shahbazi, Ali Shirali, Hamid Aghajan, and Hamed Nili. 2021. Using distance on the riemannian manifold to compare representations in brain and in models. *NeuroImage*, 239:118271.
- [36] C.G. Small. 2012. *The Statistical Theory of Shape*. Springer Series in Statistics. Springer New York.
- [37] Richard Socher, Alex Perelygin, Jean Wu, Jason Chuang, Christopher D. Manning, Andrew Ng, and Christopher Potts. 2013. Recursive deep models for semantic compositionality over a sentiment treebank. In *Proceedings of the 2013 Conference on Empirical Methods in Natural Language Processing*, pages 1631–1642, Seattle, Washington, USA. Association for Computational Linguistics.
- [38] Hrishikesh D. Vinod. 1976. Canonical ridge and econometrics of joint production. *Journal of Econometrics*, 4:147–166.
- [39] Alex Wang, Amanpreet Singh, Julian Michael, Felix Hill, Omer Levy, and Samuel R. Bowman. 2019. GLUE: A multi-task benchmark and analysis platform for natural language understanding. In the Proceedings of ICLR.
- [40] Fei Wang and Jimeng Sun. 2015. Survey on distance metric learning and dimensionality reduction in data mining. *Data Mining and Knowledge Discovery*, 29(2):534–564.
- [41] Alex H. Williams, Erin M. Kunz, Simon Kornblith, and Scott W. Linderman. 2021. Generalized shape metrics on neural representations. *Advances in neural information processing systems*, 34:4738–4750.
- [42] Peter Yianilos. 1993. Data structures and algorithms for nearest neighbor search in general metric spaces. volume 93.
- [43] Ruiqi Zhong, Dhruva Ghosh, Dan Klein, and Jacob Steinhardt. 2021. Are larger pretrained language models uniformly better? comparing performance at the instance level. In *Findings of the Association for Computational Linguistics: ACL-IJCNLP 2021*, pages 3813–3827, Online. Association for Computational Linguistics.

A Limitations

In this section, we address the limitations of this work.

Non-Linear Encoder Relationships. This work focuses solely on affine similarity between encoders, as it sufficiently fits our purpose. However, several works propose non-linear measures to capture the potentially practically relevant non-linear relationships between encoders. For instance, the MULTIBERT encoder representations are generally not exactly affinely related, which is a case discussed in §4. However, understanding the algebraic properties of the discussed similarity measures on \mathcal{E}_V still helps us to make conclusions about practical findings as in §7.

Linear Classifiers. Our work provides extrinsic theoretical guarantees for the class of linear classifiers. In practice, task fine-tuning can become as complex as re-training entire pre-trained models, which is not covered by this work. Still, we point out its utility for the class of linear probing classifiers [1, 20].

Numerical Approximations. We make several numerical approximations to move from our theoretical findings about affine homotopy relations on \mathcal{E}_V to our implementations in §7. For example, although we prove bounds for suprema and infima, we will generally not reach them exactly using gradient descent methods, as highlighted in §7. Further, although $d_{\mathcal{V}(V,\Delta)}$ is an interesting quantity to discuss, Eq. (23) is hard to optimize for numerically, and requires expensive approximation. Similarly, computing the intrinsic distances across all representation layers in Fig. 1 is done by optimizing for the MSE and evaluating the max loss, rather than directly optimizing the max loss. This is an approximation of \mathfrak{D} due to limited computational resources. Finally, we acknowledge the numerical inaccuracies when computing SVD numerically in §7, which we attempt to accommodate for using the rank to precision ϵ .

B Additional Related Work

In this section, we complement our discussion in §6 and §8 with additional related work.

Representational and Functional Similarity. Our work is related to the ongoing efforts to quantify the similarity between neural networks. The most related of which are described in §6. Many of these discuss similarity measures in terms of their invariance properties [11, 22, *inter alia*]. Klubunde et al. [21] provides a recent comprehensive overview of such. Notably, they compile various *representational* [18, 23, 27, 31, 38, *inter alia*] and *functional* similarity measures, which are related to our notions of intrinsic and extrinsic homotopy, respectively. Whereas the structure of our definition of intrinsic affine homotopy measures fits into the class of linear alignment-based measures [11, 27, 41, *inter alia*] as described in §6, our definition of extrinsic similarity fits into the broader category of performance-based functional measures [2, 7, 26]. Most relevantly, Boix-Adserà et al. [4] propose the GULP metric that provides a bound on the expected prediction dissimilarity for norm-one-bounded ridge regression.

Similarity Measures as Metrics. A line of work takes from *statistical shape analysis* [36] to motivate developing similarity measures that are proper mathematical metrics [4, 35, 41]. Learning in such proper metric spaces brings certain theoretical guarantees [3, 6, 9, 40, 42]. For example, Williams et al. [41] derive two families of so-called *generalized shape metrics* according to which they modify existing dissimilarity measures to convert them into metrics. Interestingly, one generalized shape metric is based on linear regression over the group of linear isometries, similar to what was derived for encoder maps in Prop. 3.1.

Understanding Similarity of Language Encoders. Finally, several previous works characterize the landscape of language encoders and their sensitivity to slight changes to the pre-training or fine-tuning procedure [8, 12, 43]. This prompted multi-seed releases of encoders such as BERT [34, 43] that are frequently used for robustness or sensitivity analysis [11, 32], similar to the one presented in this work.

C Addenda on Affine Homotopy

In this section, we provide additional derivations and proofs complementing the discussions in §3–§5.

C.1 Preliminaries on Hemi-Metric Spaces

Definition C.1. Let (X, d) be a hemi-metric space. The **open ball** $B(x, \varepsilon)$ of center x and radius $\varepsilon > 0$, is the set $\{y \in X \mid d(x, y) < \varepsilon\}$. The open balls form a base for the open ball topology.²⁴

Lemma 4.1. Let (X, d) be a hemi-metric space. The relation $(x \succeq_d y \text{ iff } d(x, y) = 0)$ is a **preorder**²⁵ and it will be called the **specialization ordering** of d .

Example C.1. An example of a specialization ordering is the prefix ordering of strings \leq_{prefix} .²⁶ More precisely, for any $\mathbf{y}, \mathbf{y}' \in \Sigma^*$, we define $d_{\Sigma^*}(\mathbf{y}, \mathbf{y}')$ to be zero if \mathbf{y} is a prefix of \mathbf{y}' , and to be 2^{-n} otherwise, where n is the length of the longest prefix of \mathbf{y} that is also a prefix of \mathbf{y}' . Then (Σ^*, d_{Σ^*}) is a hemi-metric space whose specialization ordering is \leq_{prefix} . //

Lemma C.1. Let (X, d) be a hemi-metric space. For every non-empty $E \subset X$, we define the map

$$d(x, E) = \inf_{y \in E} d(x, y).$$

1. The set $\{x \in X \mid d(x, E) = 0\}$ is exactly the closure of E in the open ball topology.
2. For any $x, x' \in X$, we have the inequality $d(x, E) \leq d(x, x') + d(x', E)$. If d is a metric, then $d(\cdot, E)$ is 1-Lipschitz from (X, d) to $\overline{\mathbb{R}}_+$.
3. Let $\mathcal{Z} \subset \mathcal{P}(X)$ be any space of non-empty subsets of X . The **Hausdorff-Hoare map**

$$d^{\mathcal{H}}(E, E') = \sup_{x \in E} d(x, E')$$

is hemi-metric on \mathcal{Z} . Its specialization ordering $\succeq_{d^{\mathcal{H}}}$ is given by $E \succeq_{d^{\mathcal{H}}} E'$ iff²⁷ $E \subset \text{cl}(E')$, iff $\text{cl}(E) \subset \text{cl}(E')$.

Proof. See Goubault-Larrecq [16, Lemma 6.1.11, Proposition 6.2.16 & Lemma 7.5.1]. ■

C.2 Additional Derivations: Affine Alignment Measures

Remark 3.2. We note that when $S = \text{Aff}(V)$, the map $d_{\text{Aff}(V)}(\mathbf{h}, \mathbf{g}) \stackrel{\text{def}}{=} \inf_{\psi, \psi' \in \text{Aff}(V)} \|\psi \circ \mathbf{h} - \psi' \circ \mathbf{g}\|_{\infty}$ is trivially zero by Corollary C.1. Further, $\bar{d}_{\text{Aff}(V)}$ defined in Eq. (9b) is not a metric on \mathcal{E}_V .²⁸

Proof. To see this, consider the following two encoders: $\mathbf{g}(\mathbf{y}) = |\mathbf{y}| \cdot e$, where $e \in V$ is any fixed vector, and \mathbf{h} be any map from Σ^* to the ball $B(0_V, 1)$ of radius one. In such a case, we have $\bar{d}(\mathbf{h}, \mathbf{g}) = \infty$. Even on the space of bounded encoders²⁹ $\bar{d}_{\text{Aff}(V)}$ is not a metric. We provide the following counter-example: let \mathbf{h} be any rank R encoder, e.g., \mathbf{h} can be any map that sends the first R strings to the basis of V . Let A be a non-invertible linear map of V and set $\mathbf{g} = A(\mathbf{h})$. Then clearly $\bar{d}(\mathbf{h}, \mathbf{g}) = 0$, but $\bar{d}(\mathbf{g}, \mathbf{h})$ can not be zero for dimensionality reasons (see Thm. 4.1). ■

Lemma C.2 (Hausdorff Distance). The map

$$d_{\infty}^{\mathcal{H}}(E, E') \stackrel{\text{def}}{=} \max(d_{\infty}^{\mathcal{H}}(E, E'), d_{\infty}^{\mathcal{H}}(E', E)) = \sup_{\mathbf{h} \in \mathcal{E}_V} |d_{\infty}^{\mathcal{H}}(\mathbf{h}, E) - d_{\infty}^{\mathcal{H}}(\mathbf{h}, E')|$$

is an extended pseudo-metric on $\mathcal{P}(\mathcal{E}_V) \setminus \{\emptyset\}$.

Proof. It follows readily from Lemma C.1. See also Burago et al. [5, §7.3.1]. ■

²⁴This, by definition, is the topology generated by all open balls.

²⁵A reflexive and transitive relation on X .

²⁶Defined by $\mathbf{y} \leq_{\text{prefix}} \mathbf{y}'$ if \mathbf{y} is a prefix of \mathbf{y}' .

²⁷Here, the closure is with respect to the topology defined by d .

²⁸See App. C.2 for a derivation.

²⁹Recall $\mathcal{E}_b \stackrel{\text{def}}{=} \{\mathbf{h} \in \mathcal{E}_V \mid \mathbf{h}(\Sigma^*) \text{ is bounded}\}$.

For any affine subgroup $S \subset \text{Aff}(V)$, let $S(\mathbf{h}) \stackrel{\text{def}}{=} \{\psi(\mathbf{h}) \mid \psi \in S\}$. It then follows immediately from Lemma C.2 that the map $d_S^H(\mathbf{h}, \mathbf{g}) \stackrel{\text{def}}{=} d_\infty^H(S(\mathbf{h}), S(\mathbf{g}))$ is an extended pseudo-metric on \mathcal{E}_V .

Lemma C.3. For any $\mathbf{h}, \mathbf{g} \in \mathcal{E}_V$, any $\psi \in \text{Iso}(V)$ and any non-empty $S \subset \mathcal{E}_V$, we have

$$d_S(\psi \circ \mathbf{h}, \mathbf{g}) = d_{\phi^{-1}S}(\mathbf{h}, \mathbf{g}). \quad (24)$$

In particular, $\mathfrak{d}_{\text{Iso}(V)}(\psi\mathbf{h}, \mathbf{g}) = \mathfrak{d}_{\text{Iso}(V)}(\mathbf{h}, \mathbf{g})$.

Proof. Lemma C.3 follows by definition $d_\infty(\psi \circ \mathbf{h}, \psi\mathbf{g}) = d_\infty(\mathbf{h}, \psi^{-1}\psi\mathbf{g})$. ■

Proposition 3.1. The pair $(\mathcal{E}_V, \mathfrak{d}_{\text{Iso}(V)})$ is an extended pseudo-metric space.

Proof. Using Lemma C.3, one can show that $\mathfrak{d}_{\text{Iso}(V)}(\mathbf{h}, \mathbf{g}) = d_\infty^H(\text{Iso}(\mathbf{h}), \text{Iso}(\mathbf{g}))$, where $\text{Iso}(\mathbf{h}) \stackrel{\text{def}}{=} \{\psi \circ \mathbf{h} : \psi \in \text{Iso}(V)\}$. The proposition follows then from Lemma C.2. ■

For any $\psi \in \text{Aff}(V)$ and any $\mathbf{h} \in \mathcal{E}_V$, we then have

$$\psi \circ \mathbf{h} \in \mathcal{E}_b \Leftrightarrow \mathbf{h} \in \mathcal{E}_b \Leftrightarrow \|\mathbf{h}\|_\infty < \infty.$$

Lemma C.4.

1. If $\mathbf{h} \in \mathcal{E}_b$, then

$$\|\mathbf{h}\|_{\text{Iso}(V)} = \|\mathbf{h}\|_{\mathcal{T}} = r_{\mathbf{h}},$$

where $r_{\mathbf{h}}$ denotes the radius of \mathbf{h} , which we define as the radius of the minimum enclosing ball of the set $\mathbf{h}(\Sigma^*)$.

2. For any $\psi \in \text{Aff}(V)$ and a subset $S \subset \text{Aff}(V)$ normalized by ψ and containing \mathcal{T} . Then

$$\|\psi \circ \mathbf{h}\|_S \leq \|\psi_{\text{lin}}\|_V \cdot \|\mathbf{h}\|_S.$$

Proof.

1. Let $t \in \mathcal{T}$ be the translation moving the center of the ball enclosing $\mathbf{h}(\Sigma^*)$ to the center 0_V . Hence

$$\|\mathbf{h}\|_{\text{Iso}(V)} \leq \|\mathbf{h}\|_{\mathcal{T}} \leq \|t \circ \mathbf{h}\|_\infty = r_{\mathbf{h}}$$

Now observe that for any other isometry $\psi \neq t$, then $r_{\psi \circ \mathbf{h}} = r_{\mathbf{h}}$. The ball $B(0_V, \|\psi \circ \mathbf{h}\|_\infty)$ clearly contains all points in $\psi \circ \mathbf{h}(\Sigma^*)$, hence by definition of the radius $r_{\psi \circ \mathbf{h}}$ we must have $\|\psi \circ \mathbf{h}\|_\infty \leq r_{\mathbf{h}}$, which finishes the proof of 1.

2. Write $\psi = \phi_{\text{lin}} \circ t$, with $t \in \mathcal{T}$. We then have

$$\begin{aligned} \|\psi \circ \mathbf{h}\|_S &= \inf_{\phi \in S} \|\phi(\psi \circ \mathbf{h})\|_\infty \\ &= \inf_{\phi \in S} \|\psi_{\text{lin}}(\underbrace{\psi_{\text{lin}}^{-1}\phi\psi_{\text{lin}}t}_{\in S} \circ \mathbf{h})\|_\infty \end{aligned}$$

Note that $\phi \mapsto \psi_{\text{lin}}^{-1}\phi\psi_{\text{lin}}t$ is by definition a bijection of S , hence

$$\begin{aligned} \|\psi \circ \mathbf{h}\|_S &= \inf_{\phi \in S} \|\psi_{\text{lin}}(\phi \circ \mathbf{h})\|_\infty \\ &= \inf_{\phi \in S} \sup_{\mathbf{y} \in \Sigma^*} |\psi_{\text{lin}}((\phi \circ \mathbf{h})(\mathbf{y}))|_V \\ &\leq \|\psi_{\text{lin}}\|_V \inf_{\phi \in S} \sup_{\mathbf{y} \in \Sigma^*} |(\phi \circ \mathbf{h})(\mathbf{y})|_V \\ &= \|\psi_{\text{lin}}\|_V \cdot \|\mathbf{h}\|_S. \end{aligned} \quad \blacksquare$$

Corollary C.1. Let $S \supset \mathcal{T}$. Assume that there exists $\phi \in S$ such that $\|\phi_{\text{lin}}\|_V < 1$, e.g. $S = \text{Aff}(F)$. Therefore, $d_S(\mathbf{h}, \mathbf{g}) \stackrel{\text{def}}{=} \inf_{\psi, \psi' \in S} \|\psi \circ \mathbf{h} - \psi' \circ \mathbf{g}\|_\infty = 0$ for all $\mathbf{h}, \mathbf{g} \in \mathcal{E}_b$.

Proof. Note that $\mathfrak{d}_S(\psi\mathbf{h}, \mathbf{g}) \leq \|\psi_{\text{lin}}\|_V \cdot \mathfrak{d}_S(\mathbf{h}, \mathbf{g})$, which follows from Lemma C.4. Hence

$$\begin{aligned} \mathfrak{d}_S(\mathbf{h}, \mathbf{g}) &= \inf_{\psi \in S} \mathfrak{d}_S(\psi\mathbf{h}, \mathbf{g}) \\ &\leq \underbrace{\inf_{\psi \in S} \|\psi_{\text{lin}}\|_V}_{=0} \mathfrak{d}_S(\mathbf{h}, \mathbf{g}). \end{aligned} \quad \blacksquare$$

C.3 Proofs: Intrinsic Affine Homotopy

Lemma 4.2 (Intrinsic Affine Preorder). *For any two encoders $\mathbf{h}, \mathbf{g} \in \mathcal{E}_V$, define the relation $(\mathbf{h} \succ_{\text{Aff}} \mathbf{g} \text{ iff } \mathfrak{d}_{\text{Aff}(V)}(\mathbf{h}, \mathbf{g}) = 0)$. Then \succ_{Aff} is a preorder on \mathcal{E}_V .*

Proof. Since $\mathfrak{d}_{\text{Aff}}(\psi\mathbf{h}, \mathbf{g}) \leq \|\psi\|_V \cdot \mathfrak{d}_{\text{Aff}}(\mathbf{h}, \mathbf{g})$ (see Lemma C.4),

$$\mathfrak{d}_{\text{Aff}}(\mathbf{h}, \mathbf{g}) = 0 \Leftrightarrow d_{\text{Aff}(V)}^{\mathcal{H}}(\mathbf{h}, \mathbf{g}) = 0.$$

Therefore, the relation \succ_{Aff} is the specialization ordering of the hemi-metric $d_{\text{Aff}(V)}^{\mathcal{H}}$. \blacksquare

Theorem 4.1. *Let $\mathbf{h}, \mathbf{g} \in \mathcal{E}_V$, we then have*

$$\mathbf{h} \succ_{\text{Aff}} \mathbf{g} \Leftrightarrow \mathbf{h} = \psi(\pi_{\mathbf{h}}\mathbf{g}) \text{ for some } \psi \in \text{Aff}(V) \quad (10)$$

where, $\pi_{\mathbf{h}}$ is the orthogonal projection of V onto $V_{\mathbf{h}}$. In particular, if $\mathfrak{d}_{\text{Aff}(V)}(\mathbf{h}, \mathbf{g}) = 0$ then $\text{rank}(\mathbf{h}) \leq \text{rank}(\mathbf{g})$. If in addition, we know $\text{rank}(\mathbf{g}) = \text{rank}(\mathbf{h})$, then \mathbf{g} must be an affine transformation of \mathbf{h} , i.e. $\mathbf{h} = \psi \circ \mathbf{g}$ for some $\psi \in \text{Aff}(V)$.

Proof.

1. Recall from §3.2 that \mathcal{E}_V is complete with respect to the metric $d(\cdot, \cdot)_{\infty}$. The condition $\mathfrak{d}(\mathbf{h}, \mathbf{g})_{\text{Aff}(V)} = 0$ simply means that there exists $\phi_n \in \text{Aff}(V)$ such that $\lim_{n \rightarrow \infty} \phi_n \mathbf{g} = \mathbf{h}$ in \mathcal{E}_V , in other words $\mathbf{h} \in \overline{\text{Aff}(\mathbf{g})}$, i.e. \mathbf{h} lies in the closure of $\text{Aff}(\mathbf{g})$ in \mathcal{E}_V .

Let $\mathcal{B}_{\mathbf{h}} \subset \Sigma^*$ such that $\mathbf{h}(\mathcal{B}_{\mathbf{h}})$ is a basis for $V_{\mathbf{h}}$. Therefore, there exists $\epsilon > 0$ such that any family³⁰

$$(v_{\mathbf{y}})_{\mathbf{y}} \in \prod_{\mathbf{y} \in \mathcal{B}_{\mathbf{h}}} B(\mathbf{h}(\mathbf{y}), \epsilon)$$

has $\text{rank dim}_{\mathbb{R}}(V_{\mathbf{h}})$. This shows that there exists $N \geq 1$ such that for any $n \geq N$ one has $\|\mathbf{h} - \phi_n \mathbf{g}\|_{\infty} < \epsilon$, and

$$\text{rank}(\{\phi_n \mathbf{g}(\mathbf{y}) : \mathbf{y} \in \mathcal{B}_{\mathbf{h}}\}) = \text{rank}(\mathbf{h}).$$

Which implies in particular

$$\text{dim}_{\mathbb{R}}(V_{\mathbf{h}}) \leq \text{dim}_{\mathbb{R}}(V_{\mathbf{g}}) \text{ i.e., } \text{rank } \mathbf{h} \leq \text{rank } \mathbf{g}. \quad (25)$$

2. If $\text{rank}(\mathbf{g}) = \text{rank}(\mathbf{h}) = d$, then $\lim_{n \rightarrow \infty} \phi_n = \phi$, where ϕ is the affine map given by $\mathbf{g}(\mathbf{y}) \mapsto \mathbf{h}(\mathbf{y})$ for $\mathbf{y} \in \mathcal{B}_{\mathbf{h}}$. Indeed, for any $v = \sum_{b \in \mathcal{B}_{\mathbf{h}}} \lambda_b b \in V$, we have

$$\|(\phi - \phi_n)(v)\| \leq \|\mathbf{h} - \psi_n \mathbf{g}\|_{\infty} \sum_{b \in \mathcal{B}_{\mathbf{h}}} |\lambda_b| \leq c \|\mathbf{h} - \psi_n \mathbf{g}\|_{\infty} \|v\|_V$$

for some constant $c > 0$, since all norms on V are equivalent. Hence, $\lim_{n \rightarrow \infty} \|\phi - \phi_n\|_V = 0$, which shows the claim. Accordingly, we must have $\phi(\mathbf{g}) = \mathbf{h}$.

Now we can prove Eq. (10):

- 3 \Rightarrow . Given that $\|\mathbf{h} - \pi_{\mathbf{h}} \circ \phi_n(\mathbf{g})\|_{\infty} \leq \|\mathbf{h} - \phi_n \mathbf{g}\|_{\infty}$, we also have $\lim_{n \rightarrow \infty} \pi_{\mathbf{h}} \circ \phi_n(\mathbf{g}) = \mathbf{h}$.

Write π^{\perp} for the orthogonal projection on V^{\perp} and set $\pi_{\mathbf{h},n} = \pi_{\mathbf{h}} \oplus \frac{1}{n\|\phi_n\|} \pi_{\mathbf{h}}^{\perp}$. Note that $\lim_{n \rightarrow \infty} \pi_{\mathbf{h},n} = \pi_{\mathbf{h}}$. Accordingly,

$$\lim_{n \rightarrow \infty} \psi_n(\pi_{\mathbf{h}} \mathbf{g}) = \mathbf{h},$$

where $\psi_n = \pi_{\mathbf{h},n} \phi_n \pi_{\mathbf{h},n}^{-1}$. From which we deduce that

$$\mathfrak{d}_{\text{Aff}(V)}(\mathbf{h}, \pi_{\mathbf{h}} \mathbf{g}) = 0.$$

Now applying 2. yields $\mathbf{h} = \phi(\pi_{\mathbf{h}} \mathbf{g})$ for some $\phi \in \text{Aff}(V_{\mathbf{h}})$, or $\mathbf{h} = \phi(\pi_{\mathbf{h}} \mathbf{g})$ where $\phi = \phi_h \oplus \pi_{\mathbf{h}}^{\perp} \in \text{Aff}(V)$.

- 3 \Leftarrow . Assume now that $\mathbf{h} = \phi(\pi_{\mathbf{h}} \mathbf{g})$ for some $\phi \in \text{Aff}(V)$. Then $\mathbf{h} = \lim_{n \rightarrow \infty} \phi \circ \pi_{\mathbf{h},n}(\mathbf{g})$, where $\pi_{\mathbf{h},n} = \pi_{\mathbf{h}} \oplus \frac{1}{n} \pi_{\mathbf{h}}^{\perp}$, which shows the desired implication. \blacksquare

³⁰close enough to $\mathbf{h}(\mathcal{B}_{\mathbf{h}})$.

C.4 Proofs: Extrinsic Homotopy

Lemma 5.1. *Let $\mathbf{h}, \mathbf{g} \in \mathcal{E}_V$. We have*

1. *There exists a constant $c(\lambda) > 0$ such that for any $\psi \in \text{Aff}(V, W)$*

$$d_{\infty, \Delta^{N-1}}(\text{softmax}_\lambda(\psi \circ \mathbf{h}), \mathcal{V}_N(\mathbf{g})) \leq c(\lambda) \|\psi_{\text{lin}}\| \mathfrak{d}_{\text{Aff}(V)}(\mathbf{h}, \mathbf{g}).$$

2. $d_{\mathcal{V}(V, \Delta)}(\mathbf{h}, \mathbf{g}) \leq c(\lambda) d_{\text{Aff}(V, W)}(\mathbf{h}, \mathbf{g})$.

3. $\mathfrak{d}_{\text{Aff}(V)}(\mathbf{h}, \mathbf{g}) = 0 \Rightarrow d_{\text{Aff}(V, W)}(\mathbf{h}, \mathbf{g}) = 0 \Rightarrow d_{\mathcal{V}(V, \Delta)}(\mathbf{h}, \mathbf{g}) = 0$.

Proof.

1. Clearly,

$$\begin{aligned} d_{\infty, \Delta^{N-1}}(\text{softmax}_\lambda \psi \circ \mathbf{h}, \mathcal{V}_N(\mathbf{g})) &\leq c(\lambda) d_{\infty, W}(\psi \circ \mathbf{h}, \text{Aff}_{V, W}(\mathbf{g})) \\ &\leq c(\lambda) \inf_{\psi' \in \psi \circ \text{Aff}(V)} \|\psi \circ \mathbf{h} - \psi' \circ \mathbf{g}\|_{\infty, W} \\ &= c(\lambda) \inf_{\psi' \in \text{Aff}(V)} \|\psi(\mathbf{h} - \psi' \circ \mathbf{g})\|_{\infty, W} \\ &= c(\lambda) \|\psi_{\text{lin}}\| \mathfrak{d}_{\text{Aff}(V)}(\mathbf{h}, \mathbf{g}). \end{aligned}$$

where, the first inequality follows from the fact that softmax_λ is $c(\lambda)$ -Lipschitz for some constant that depends on λ [15, Proposition 4].

2. & 3. are immediate consequences of 1. ■

Theorem 5.1 (ε -Intrinsic $\Rightarrow \mathcal{O}(\varepsilon)$ -Extrinsic). *Let $\mathbf{h}, \mathbf{g} \in \mathcal{E}_V$ be two encoders. Then,*

$$d_{\mathcal{V}(V, \Delta)}(\mathbf{h}, \mathbf{g}) \leq c(\lambda) d_{\text{Aff}(V)}^{\mathcal{H}}(\mathbf{h}, \mathbf{g}).$$

Proof. Let $\psi \in \text{Aff}(V, W)$. There exists a linear map $A: V \rightarrow W$ and a $\phi_V \in \text{GL}(V)$, such that $\psi = A \circ \phi$ and $\|A\| = 1$. Accordingly, Lemma 5.1 yields

$$d_{\infty, \Delta^{N-1}}(\text{softmax}_\lambda(\psi \circ \mathbf{h}), \mathcal{V}_N(\mathbf{g})) \leq c(\lambda) d_{\infty, W}(\psi \circ \mathbf{h}, \text{Aff}_{V, W}(\mathbf{g})) \quad (27)$$

$$\leq c(\lambda) \mathfrak{d}_{\text{Aff}(V)}(\phi_V \circ \mathbf{h}, \mathbf{g}) \quad (28)$$

$$\leq c(\lambda) \sup_{\psi_V \in \text{Aff}(V)} (\mathfrak{d}_{\text{Aff}(V)}(\psi_V \circ \mathbf{h}, \mathbf{g})) \quad (29)$$

$$= c(\lambda) d_{\text{Aff}(V)}^{\mathcal{H}}(\mathbf{h}, \mathbf{g}). \quad (30)$$

Therefore $d_{\mathcal{V}(V, \Delta)}(\mathbf{h}, \mathbf{g}) \leq c(\lambda) d_{\text{Aff}(V)}^{\mathcal{H}}(\mathbf{h}, \mathbf{g})$. ■

D Proofs: Linear Alignment Methods for Finite Representation Sets

Linear Regression Let $\mathbf{H} \in \mathbb{R}^{N \times d}$ and $\mathbf{G} \in \mathbb{R}^{N \times d}$ be two representation matrices. A straightforward related way to evaluate the similarity of two representation spaces is through linear regression. Linear regression finds the matrix $\hat{\mathbf{A}} \in \mathbb{R}^{d \times d}$ that minimizes the least squares error

$$\hat{\mathbf{A}} = \underset{\mathbf{A} \in \mathbb{R}^{d \times d}}{\text{argmin}} \|\mathbf{G} - \mathbf{H}\mathbf{A}\|_F^2, \quad (31)$$

for which we can find an exact solution in $(\mathbf{H}^\top \mathbf{H})^{-1} \mathbf{H}^\top \mathbf{G}$. Let $\mathbf{H} = \mathbf{Q}_\mathbf{H} \mathbf{R}_\mathbf{H}$ and $\mathbf{G} = \mathbf{Q}_\mathbf{G} \mathbf{R}_\mathbf{G}$ be the QR-decomposition of \mathbf{H} and \mathbf{G} , respectively. The goodness of fit is commonly evaluated through the R-squared value R_{LR}^2 , i.e., as the proportion of variance in \mathbf{G} explained by the fit:

$$R_{LR}^2 = 1 - \frac{\|\mathbf{G} - \mathbf{H}\hat{\mathbf{A}}\|_F^2}{\|\mathbf{G}\|_F^2} = \frac{\|\mathbf{Q}_\mathbf{G}^\top \mathbf{H}\|_F^2}{\|\mathbf{G}\|_F^2}. \quad (32)$$

The exact minimum of Eq. (32) is reached at $\hat{\mathbf{A}} = (\mathbf{H}^\top \mathbf{H})^{-1} \mathbf{H}^\top \mathbf{G}$. The fitted values $\hat{\mathbf{G}}$ are

$$\begin{aligned}\hat{\mathbf{G}} &= \mathbf{H}\hat{\mathbf{A}} = \mathbf{H}(\mathbf{H}^\top \mathbf{H})^{-1} \mathbf{H}^\top \mathbf{G} \\ &= \mathbf{Q}_\mathbf{H} \mathbf{R}_\mathbf{H} (\mathbf{R}_\mathbf{H}^\top \mathbf{Q}_\mathbf{H}^\top \mathbf{Q}_\mathbf{H} \mathbf{R}_\mathbf{H})^{-1} \mathbf{R}_\mathbf{H}^\top \mathbf{Q}_\mathbf{H}^\top \mathbf{G} \\ &= \mathbf{Q}_\mathbf{H} \mathbf{Q}_\mathbf{H}^\top \mathbf{G}\end{aligned}$$

The residuals are therefore

$$\begin{aligned}\|\mathbf{G} - \hat{\mathbf{G}}\|_F^2 &= \text{tr}((\mathbf{G} - \hat{\mathbf{G}})^\top (\mathbf{G} - \hat{\mathbf{G}})) && \text{(residuals orthogonal to fitted values)} \\ &= \text{tr}((\mathbf{G} - \hat{\mathbf{G}})^\top \mathbf{G}) \\ &= \text{tr}(\mathbf{G}^\top \mathbf{G}) - \text{tr}(\mathbf{G}^\top \mathbf{Q}_\mathbf{H} \mathbf{Q}_\mathbf{H}^\top \mathbf{G}) \\ &= \|\mathbf{G}\|_F^2 - \|\mathbf{Q}_\mathbf{H}^\top \mathbf{G}\|_F^2\end{aligned}$$

We can finally compute the coefficient of determination as

$$R_{LR}^2 = 1 - \frac{\|\mathbf{G} - \hat{\mathbf{G}}\|_F^2}{\|\mathbf{G}\|_F^2} = 1 - \frac{\|\mathbf{G}\|_F^2 - \|\mathbf{Q}_\mathbf{H}^\top \mathbf{G}\|_F^2}{\|\mathbf{G}\|_F^2} = \frac{\|\mathbf{Q}_\mathbf{H}^\top \mathbf{G}\|_F^2}{\|\mathbf{G}\|_F^2}.$$

Orthogonal Procrustes Problem. Let $\mathbf{G} \in \mathbb{R}^{N \times d}$ and $\mathbf{H} \in \mathbb{R}^{N \times d}$ two finite sets of representations. In the orthogonal Procrustes problem, we seek to find the orthogonal matrix \mathbf{A} that best maps \mathbf{H} to \mathbf{G}

$$\hat{\mathbf{A}} = \underset{\mathbf{A}}{\text{argmin}} \|\mathbf{G} - \mathbf{H}\mathbf{A}\|_F, \quad \text{subject to } \mathbf{A}^\top \mathbf{A} = \mathbb{I} \quad (33)$$

Since

$$\begin{aligned}\|\mathbf{G} - \mathbf{H}\mathbf{A}\|_F^2 &= \text{tr}((\mathbf{G} - \mathbf{H}\mathbf{A})^\top (\mathbf{G} - \mathbf{H}\mathbf{A})) \\ &= \text{tr}(\mathbf{G}^\top \mathbf{G}) - \text{tr}(\mathbf{G}^\top \mathbf{H}\mathbf{A}) - \text{tr}(\mathbf{A}^\top \mathbf{H}^\top \mathbf{G}) + \text{tr}(\mathbf{A}^\top \mathbf{H}^\top \mathbf{H}\mathbf{A}) \\ &= \|\mathbf{G}\|_F^2 + \|\mathbf{H}\|_F^2 - 2\text{tr}(\mathbf{A}^\top \mathbf{H}^\top \mathbf{G}),\end{aligned}$$

an equivalent objective to Eq. (20) is

$$\hat{\mathbf{A}} = \underset{\mathbf{A}}{\text{argmax}} \langle \mathbf{A}\mathbf{H}, \mathbf{G} \rangle_F \quad \text{subject to } \mathbf{A}^\top \mathbf{A} = \mathbb{I}.$$

Let $\mathbf{U}\Sigma\mathbf{V}^\top$ be the singular-value decomposition of $\mathbf{H}^\top \mathbf{G}$, then

$$\begin{aligned}\hat{\mathbf{A}} &= \underset{\mathbf{A}}{\text{argmax}} \langle \mathbf{A}, \mathbf{G}\mathbf{H}^\top \rangle_F \\ &= \underset{\mathbf{A}}{\text{argmax}} \langle \mathbf{A}, \mathbf{G}\mathbf{H}^\top \rangle_F \\ &= \underset{\mathbf{A}}{\text{argmax}} \langle \mathbf{A}, \mathbf{U}\Sigma\mathbf{V}^\top \rangle_F \\ &= \underset{\mathbf{A}}{\text{argmax}} \langle \mathbf{U}^\top \mathbf{A}\mathbf{V}, \Sigma \rangle_F\end{aligned}$$

where $\mathbf{U}^\top \mathbf{A}\mathbf{V}$ is a product of orthogonal matrices, and, therefore, orthogonal. This means that we find the maximum for $\mathbf{U}^\top \mathbf{A}\mathbf{V} = \mathbb{I}$, i.e., $\mathbb{I} = \mathbf{U}^\top \hat{\mathbf{A}}\mathbf{V}$, which finally yields $\hat{\mathbf{A}} = \mathbf{U}\mathbf{V}^\top$.

Canonical Correlation Analysis. We can rewrite the general CCA objective in Eq. (21) as

$$\max_{\mathbf{A}, \mathbf{B}} \text{tr}(\mathbf{A}^\top \mathbf{H}\mathbf{G}^\top \mathbf{B}) \quad \text{s.t.} \quad (\mathbf{A}^\top \mathbf{H})(\mathbf{A}^\top \mathbf{H})^\top = (\mathbf{B}^\top \mathbf{G})(\mathbf{B}^\top \mathbf{G})^\top = \mathbb{I}, \quad (34)$$

which, by definition of the Frobenius norm, is equivalent to optimizing

$$\min_{\mathbf{A}, \mathbf{B}} \frac{1}{2} \|\mathbf{A}^\top \mathbf{H} - \mathbf{B}^\top \mathbf{G}\|_F^2 \quad \text{s.t.} \quad (\mathbf{A}^\top \mathbf{H})(\mathbf{A}^\top \mathbf{H})^\top = (\mathbf{B}^\top \mathbf{G})(\mathbf{B}^\top \mathbf{G})^\top = \mathbb{I}. \quad (35)$$

Let $\mathbf{M}_{\mathbf{H}\mathbf{G}} = \mathbf{H}\mathbf{G}^\top$, $\mathbf{M}_{\mathbf{H}\mathbf{H}} = \mathbf{H}\mathbf{H}^\top$, and $\mathbf{M}_{\mathbf{G}\mathbf{G}} = \mathbf{G}\mathbf{G}^\top$. Further, let $\mathbf{U}\Sigma\mathbf{V}^\top$ be the singular-value decomposition of $\mathbf{M}_{\mathbf{H}\mathbf{G}}$. We can show that the optimum of Eq. (22) is found at $(\hat{\mathbf{A}}, \hat{\mathbf{B}}) =$

$(\mathbf{M}_{\mathbf{H}\mathbf{H}}^{-\frac{1}{2}}\mathbf{U}, \mathbf{M}_{\mathbf{G}\mathbf{G}}^{-\frac{1}{2}}\mathbf{V})$. Because $\mathbf{A}^\top\mathbf{H}$, $\mathbf{B}^\top\mathbf{G}$, \mathbf{U} , and \mathbf{V} are by definition orthogonal we can conclude that CCA first whitens the representations (\mathbf{H}, \mathbf{G}) through $(\mathbf{M}_{\mathbf{H}\mathbf{H}}^{-\frac{1}{2}}, \mathbf{M}_{\mathbf{G}\mathbf{G}}^{-\frac{1}{2}})$, and then performs an orthogonal transformation. We note that for pre-whitened representation matrices, formulation Eq. (35) is equivalent to Eq. (33). To see this, let \mathbf{W}_h and \mathbf{W}_g be whitening transforms for \mathbf{H} and \mathbf{G} , respectively. Further, let $O(V)$ be the set of orthogonal $d \times d$ matrices. Eq. (35) is then equivalent to

$$\min_{\mathbf{A}, \mathbf{B} \in O(V)} \|\mathbf{A}^\top\mathbf{W}_h\mathbf{H} - \mathbf{B}^\top\mathbf{W}_g\mathbf{G}\|_F^2 \quad (36)$$

as the whitening constraints impose orthogonality constraints for \mathbf{A} and \mathbf{B}

$$(\mathbf{A}\mathbf{W}_h\mathbf{H})(\mathbf{A}\mathbf{W}_h\mathbf{H})^\top = \mathbf{A}\mathbf{A}^\top = \mathbb{I}, \quad (37)$$

$$(\mathbf{B}\mathbf{W}_g\mathbf{G})(\mathbf{B}\mathbf{W}_g\mathbf{G})^\top = \mathbf{B}\mathbf{B}^\top = \mathbb{I}, \quad (38)$$

and,

$$\begin{aligned} \min_{\mathbf{A}, \mathbf{B} \in O(V)} \|\mathbf{A}^\top\mathbf{W}_h\mathbf{H} - \mathbf{B}^\top\mathbf{W}_g\mathbf{G}\|_F^2 &= \min_{\mathbf{A}\mathbf{B}^\top \in O(V)} \|\mathbf{A}^\top\| \|\mathbf{W}_h\mathbf{H} - \mathbf{A}\mathbf{B}^\top\mathbf{W}_g\mathbf{G}\|_F^2 \quad (\mathbf{A} \in O(V)) \\ &= \min_{\mathbf{C} \in O(V)} \|\mathbf{W}_h\mathbf{H} - \mathbf{C}^\top\mathbf{W}_g\mathbf{G}\|. \quad (\mathbf{C} \stackrel{\text{def}}{=} \mathbf{A}\mathbf{B}^\top \in O(V)) \end{aligned}$$

E Experimental Setup

In this section, we provide additional details about the setup and compute resources of the experiments in §7. To generate MULTIBERT embeddings, we used the open-sourced code by Ren et al. [32]. Further, to compute Orthogonal Procrustes, CCA, PWCCA, and Linear CKA, we use the open source implementation by Ding et al. [11]. Our complete code is added as supplementary material.

Models and Datasets. We first extract the $d = 768$ dimensional training set representations for both MRPC and SST-2 across all 12 layers of the 25 MULTIBERT [34] models from HuggingFace.³¹ The models and the MRPC dataset are licensed under Apache License 2.0. The SST-2 dataset is licensed under the Creative Commons CC0: Public Domain license. The dataset statistics are shown in Tab. 3.

Dataset	Task	Train Dataset Size	Domain
SST-2	Sentiment Analysis	67K	Movie reviews
MRPC	Paraphrase Detection	3.7K	News

Table 3: Dataset statistics from the GLUE benchmark [39].

Hyperparameters. Each experiment was run using RiemannSGD³² as an optimizer as it initially produced the best convergence when computing our affine similarity measures. Further, to account for convergence artifacts, we ran the intrinsic similarity computation optimizations in each experiment for learning rates $[1\text{E-}4, 1\text{E-}3, 1\text{E-}2, 1\text{E-}1]$ and extrinsic computations for $[1\text{E-}3, 1\text{E-}2, 2\text{E-}2]$ and report the best result. When training the task-specific linear probing classifier ψ' for $\mathcal{D}_{\psi'}$, we use the cross-entropy loss, RiemannSGD and optimize over the learning rates $[1\text{E-}2, 1\text{E-}1, 2\text{E-}1, 4\text{E-}1]$. For the computation of Hausdorff-Hoare map $\mathcal{D}^{\mathcal{H}}$, we fixed a lr of $1\text{E-}3$ to save compute resources, as this lr generally leads to the best convergence in previous experiments. We chose a batch size 64 and let optimization run for 20 epochs, keeping other parameters at default. For reproducibility, we set the initial seed to 42 during training.

Generating Random Affine Maps. For the last experiment, we generate random affine maps. To approximate $\mathcal{D}^{\mathcal{H}}$ we sample the matrix entries of the affine map from $\mathcal{N}(0, 1)$. We then additionally normalize the transformed representation matrix as this leads to better convergence. To approximate $\mathcal{D}^{\mathcal{H}}$, we fit a linear probe on \mathbf{H} to 100 and 1000 sets of randomly generated class labels, for SST-2 and MRPC, respectively. The predictions of that probe then become what \mathbf{G} affinely maps to. In both cases, the seeds are set ascendingly from 0.

³¹<https://huggingface.co/google>

³²<https://github.com/geopt/geopt>

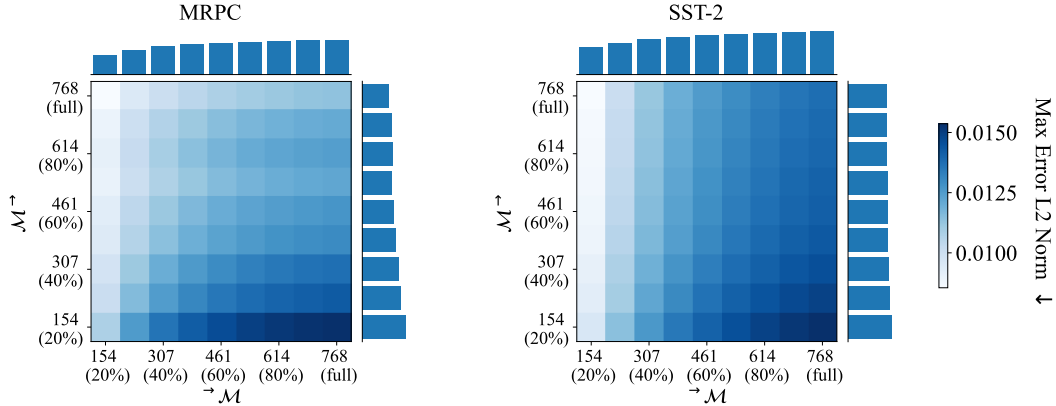


Figure 3: The effect of artificial rank deficiency averaged across MULTIBERTs. For each pair of embeddings $\mathbf{H}^{(i)}$ and $\mathbf{H}^{(j)}$ from MULTIBERTs $\mathcal{M}^{(i)}$ and $\mathcal{M}^{(j)}$ we generate additional rank-deficient encoders $\mathbf{H}_{X\%}^{(i)}$ and $\mathbf{H}_{Y\%}^{(j)}$ with $X, Y \in \{20\%, \dots, 90\%\}$ of the full rank through SVD truncation. We compute $\mathfrak{D}(\mathbf{H}_{Y\%}^{(i)}, \mathbf{H}_{X\%}^{(j)})$, for each pair of possible rank-deficiency and finally report the median across all MULTIBERTs on row X and column Y on the grid. We additionally show row-, and column medians.

Compute Resources. We compute the embeddings on a single A100-40GB GPU, which took around two hours. All other experiments were run on 8-32 CPU cores, each with 8 GB of memory. Computing extrinsic distances between 600 model combinations across both datasets usually takes 2-3 hours on 8 cores, whereas intrinsic computation is more costly, and can run up to 4 hours. Note our approximation of Hausdorff-Hoare maps (cf. Eq. (23)) across all models is significantly more costly due to our sampling approach and can take up to 72 hours to compute on 32 cores for large datasets such as SST-2, and up to 12 hours for MRPC. The compute needed for initially failed experiments do not significantly exceed the reported compute.

F Additional Experimental Results

The Influence of Encoder Rank Deficiency. In Thm. 4.1 we discuss how the relative rank of encoders influences their affine alignment. We further derive the equivalence relation \simeq_{Aff} conditioned on equal rank between encoders. To test the effect of unequal rank on affine alignment in an isolated setup, we artificially construct reduced-rank encoders through singular value decomposition (SVD) truncation. In Figure 3 we expectedly find a trend in how the encoder rank influences affine mappability. We additionally highlight that the computed distances are rather symmetric, with no clear differences when mapping *to* ($\rightarrow \mathcal{M}$), rather than *from* ($\mathcal{M} \rightarrow$) an encoder. Finally, we note the trend in the diagonal indicating that mapping between encoders of the same rank becomes easier between lower-rank encoders.